Computers and Mathematics with Applications 67 (2014) 966–995

Contents lists available at ScienceDirect

Computers and Mathematics with Applications

journal homepage: www.elsevier.com/locate/camwa

The DPG method for the Stokes problem

Nathan V. Roberts *, Tan Bui-Thanh, Leszek Demkowicz

Institute for Computational Engineering and Sciences, The University of Texas at Austin, Austin, TX 78712, USA

ARTICLE INFO

Keywords:
Discontinuous Petrov–Galerkin
Stokes problem

ABSTRACT

We discuss well-posedness and convergence theory for the DPG method applied to a general system of linear Partial Differential Equations (PDEs) and specialize the results to the classical Stokes problem. The Stokes problem is an iconic troublemaker for standard Bubnov–Galerkin methods; if discretizations are not carefully designed, they may exhibit non-convergence or locking. By contrast, DPG does not require us to treat the Stokes problem in any special manner. We illustrate and confirm our theoretical convergence estimates with numerical experiments.

1. Introduction

In this paper, we apply the Discontinuous Petrov–Galerkin (DPG) with optimal test functions methodology recently developed by Demkowicz and Gopalakrishnan [1,2] to the Stokes problem, and analyze its well-posedness. Our analysis is corroborated by numerical experiments.

The discontinuous Petrov–Galerkin method with optimal test functions. We begin with a short historical review of the method. By a discontinuous Galerkin (DG) method, we mean one that allows test and/or trial functions that are not globally conforming; by a Petrov–Galerkin method, we mean one that allows the test and trial spaces to differ. In 2002, Bottasso et al. introduced a method [3,4], also called DPG. Like our DPG method, theirs used an "ultra-weak" variational formulation (moving all derivatives to test functions) and replaced the numerical fluxes used in DG methods to "glue" the elements together with new independent unknowns defined on element interfaces. The idea of optimal testing was introduced by Demkowicz and Gopalakrishnan in 2009 [1], which is distinguished by an on-the-fly computation of an approximation to a set of test functions that are optimal in the sense that they guarantee minimization of the residual in the dual norm. In 2009–2010, a flurry of numerical experimentation followed, including applications to convection-dominated diffusion [2], wave propagation [5], elasticity [6], thin-body (beam and shell) problems [7], and the Stokes problem [8]. The wave propagation paper also introduced the concept of an *optimal test norm*, whose selection makes the energy norm identical to the norm of interest on the trial space. In 2010, Demkowicz and Gopalakrishnan proved the convergence of the method for the Laplace equation [9], and Demkowicz and Heuer developed a systematic approach to the selection of a test space norm for singularly perturbed problems [10]. In 2011, Bui-Thanh et al. [11] developed a unified analysis of DPG problems by means of Friedrichs' systems, upon which we rely for our present analysis of the Stokes problem.

Some work has been done on nonlinear problems as well. Very early on, Chan, Demkowicz, and Roberts solved the 1D Burgers and compressible Navier–Stokes equations by applying DPG to the linearized problem [12]. More recently, Moro et al. have applied their related HDPG method to the 2D Burgers equation; a key difference in their work is that they apply DPG to the *nonlinear* problem, using optimization techniques to minimize the DPG residual.

Most DPG analysis assumes that the optimal test functions are computed exactly, but in practice we must approximate them. Gopalakrishnan and Qiu have shown that for the Laplace equation and linear elasticity, for sufficiently high-order

* Corresponding author.
E-mail addresses: nroberts@ices.utexas.edu, nate@nateroberts.com (N.V. Roberts).

0898-1221/$ – see front matter
http://dx.doi.org/10.1016/j.camwa.2013.12.015

approximations[1] of the test space, optimal h-convergence rates are maintained [13]. In this work, we assume that the error in resolving the optimal test functions is negligible.

We will now briefly derive DPG, motivating it as a minimum residual method. Suppose that U is the trial space, and V the test space (both Hilbert) for a well-posed variational problem $b(u, v) = l(v)$. Writing this in the operator form $Bu = l$, where $B : U \to V'$, we seek to minimize the residual for the discrete space $U_h \subset U$:

$$u_h = \arg\min_{u_h \in U_h} \frac{1}{2} \|Bu_h - l\|^2_{V'}.$$

Now, the dual space V' is not especially easy to work with; we would prefer to work with V itself. Recalling that the Riesz operator $R_V : V \to V'$ defined by

$$\langle R_V v, \delta v\rangle = (v, \delta v)_V, \quad \forall \delta v \in V,$$

where $\langle\cdot,\cdot\rangle$ denotes the duality pairing between V' and V, is an *isometry* – that is, $\|R_V v\|_{V'} = \|v\|_V$ – we can rewrite the term we want to minimize as a norm in V:

$$\frac{1}{2}\|Bu_h - l\|^2_{V'} = \frac{1}{2}\left\|R_V^{-1}(Bu_h - l)\right\|^2_V = \frac{1}{2}\left(R_V^{-1}(Bu_h - l), R_V^{-1}(Bu_h - l)\right)_V. \tag{1.1}$$

The first-order optimality condition requires that the Gâteaux derivative of (1.1) be equal to zero for minimizer u_h; we have

$$\left(R_V^{-1}(Bu_h - l), R_V^{-1}B\delta u_h\right)_V = 0, \quad \forall \delta u_h \in U_h. \tag{1.2}$$

By the definition of R_V, the preceding equation is equivalent to

$$\langle Bu_h - l, R_V^{-1}B\delta u_h\rangle = 0 \quad \forall \delta u_h \in U_h. \tag{1.3}$$

Now, if we identify $v_{\delta u_h} = R_V^{-1}B\delta u_h$ as a test function,[2] we can rewrite (1.3) as

$$b(u_h, v_{\delta u_h}) = l(v_{\delta u_h}).$$

Note that the last equation is exactly the original variational form, tested with a special function $v_{\delta u_h}$ that corresponds to $\delta u_h \in U_h$; we call $v_{\delta u_h}$ an *optimal test function*. The DPG method is then to solve the problem $b(u_h, v_{\delta u_h}) = l(v_{\delta u_h})$ with optimal test functions $v_{\delta u_h} \in V$ that solve the problem

$$(v_{\delta u_h}, \delta v)_V = \langle R_V v_{\delta u_h}, \delta v\rangle = \langle B\delta u_h, \delta v\rangle = b(\delta u_h, \delta v), \quad \forall \delta v \in V. \tag{1.5}$$

In standard conforming methods, test functions are continuous over the entire domain, which would mean that solving (1.5) would require computations on the global mesh, making the method impractical. In DPG, we use test functions that are discontinuous across elements, so that (1.5) becomes a local problem—that is, it can be solved element-by-element. Of course, (1.5) still requires inversion of the infinite-dimensional Riesz map, and we approximate this by using an "enriched" test space V_h of polynomial order higher than that of the trial space U_h. Note that the test functions $v_{\delta u_h}$ immediately give rise to a hermitian positive definite stiffness matrix; if $\{e_i\}$ is a basis for U_h, we have:

$$b(e_i, v_{e_j}) = (v_{e_i}, v_{e_j})_V = \overline{(v_{e_j}, v_{e_i})_V} = \overline{b(e_j, v_{e_i})}.$$

It should be pointed out that we have not made any assumptions about the inner product on V. An important point is that by an appropriate choice of test space inner product, the induced energy norm on the trial space can be made to coincide with the norm of interest [5]; DPG then delivers the best approximation error in that norm. In practice this optimal test

[1] $k_{\text{test}} = k_{\text{trial}} + N$, where N is the number of space dimensions, and by k_{test} we mean the polynomial order of the basis functions for the test space, and by k_{trial} we mean the order for the L^2 bases in the trial space.

[2] A different approach has been proposed by Dahmen et al. in [14]. Instead of "taking out" the second Riesz operator in (1.2), we introduce the error representation function:

$$\psi = R_V^{-1}(Bu_h - l)$$

and reduce (1.2) to a mixed problem:

$$\begin{cases} \psi \in V, u_h \in U_h \\ (\psi, \delta\psi)_V - b(u_h, \delta\psi) = -l(\delta\psi) \quad \forall \delta\psi \in V \\ b(\delta u_h, \psi) = 0 \quad \forall \delta u_h \in U_h. \end{cases} \tag{1.4}$$

If ψ comes from a broken test space (is approximated with enriched broken spaces) and the test norm is localizable, ψ can be statically condensed at the element level and we obtain exactly the method proposed in [2]. If, however, ψ is approximated with an enriched globally conforming space, the mixed problem has to be solved using a different technique.

space inner product is approximated by a "localizable" inner product, and DPG delivers the best approximation error up to a mesh-independent constant. That is,

$$\|u - u_h\|_U \leq \frac{M}{\gamma_{\text{DPG}}} \inf_{w_h \in U_h} \|u - w_h\|_U ,$$

where $M = O(1)$ and γ_{DPG} is mesh-independent, and γ_{DPG} is of the order of inf–sup constants for the strong operator and its adjoint (see Section 2.3). We therefore say that DPG is *automatically stable*, modulo any error in solving for the test functions $v_{\delta u_h}$.

DPG also provides a precise measurement of the error in the dual norm:

$$\|Bu_h - l\|_{V'} = \left\|R_V^{-1}(Bu_h - l)\right\|_V .$$

If we then define an error representation function $e = R_V^{-1}(Bu_h - l) \in V$, we can solve

$$(e, \delta v)_V = b(u_h, \delta v) - l(\delta v), \quad \forall \delta v \in V,$$

locally for e. We use $\|e_K\|_V = \|Bu_h - l\|_{V'(K)}$ on each element K to drive adaptive mesh refinements.

It is a relatively simple matter, when desired, to enforce *local conservation* – that is, an element-wise property that corresponds to a (mass) conservation law – by means of Lagrange multipliers. This was first noted by Moro et al. [15]. This is often useful in the context of practical fluid problems, but falls outside the scope of our present analysis. In the context of the numerical examples presented here, local conservation appears to have negligible effect.

The Stokes problem. The classical strong form of the Stokes problem in $\Omega \subset \mathbb{R}^2$ is given by

$$-\mu \Delta \boldsymbol{u} + \nabla p = \boldsymbol{f} \quad \text{in } \Omega, \tag{1.6a}$$

$$\nabla \cdot \boldsymbol{u} = g \quad \text{in } \Omega, \tag{1.6b}$$

$$\boldsymbol{u} = \boldsymbol{u}_D \quad \text{on } \partial\Omega, \tag{1.6c}$$

where μ is viscosity, p pressure, $\boldsymbol{u}$ velocity, and $\boldsymbol{f}$ a vector forcing function. The first equation corresponds to conservation of momentum, and the second to conservation of mass. While the analysis will treat the case where mass can be added or removed from the system ($g \neq 0$), in practice generally (and in our numerical experiments) $g = 0$. Since by appropriate non-dimensionalization we can eliminate the constant μ, we take $\mu = 1$ throughout.

In order to apply the DPG method, we need to cast the system (1.6a)–(1.6c) as a first-order system. We introduce $\boldsymbol{\sigma} = \nabla \boldsymbol{u}$:

$$-\nabla \cdot \boldsymbol{\sigma} + \nabla p = \boldsymbol{f} \quad \text{in } \Omega, \tag{1.7a}$$

$$\nabla \cdot \boldsymbol{u} = g \quad \text{in } \Omega, \tag{1.7b}$$

$$\boldsymbol{\sigma} - \nabla \boldsymbol{u} = 0 \quad \text{in } \Omega, \tag{1.7c}$$

$$\boldsymbol{u} = \boldsymbol{u}_D \quad \text{on } \partial\Omega. \tag{1.7d}$$

Clearly, the first-order formulation is by no means unique; we have chosen this one for convenience of mathematical analysis and simplicity of presentation. Previously, we have experimented with other formulations; the velocity–stress–pressure (VSP) and velocity–vorticity–pressure (VVP) formulations [8,16]. Note also that $\boldsymbol{\sigma}$ in this formulation is *not* the physical stress (the physical stress does enter the VSP formulation).

The Stokes equations model incompressible viscous ("creeping") flow; they can be derived by neglecting the convective term in the incompressible Navier–Stokes equations. Naive discretizations for the Stokes problem can lead to non-convergence or locking [17]. Of crucial importance for Bubnov–Galerkin formulations of the Stokes equations – and more generally, of saddle point problems – is the satisfaction of the two so-called Brezzi inf–sup conditions [18]. For the Stokes equations, the first of these, the "inf–sup in the kernel" condition, is satisfied automatically. If the discrete spaces for velocity $\boldsymbol{u}$ and pressure p are $\boldsymbol{V}_h \subset \boldsymbol{H}^1$ and $Q_h \subset L^2$, respectively, the second Brezzi condition for Stokes is then

$$\inf_{q \in Q_h} \sup_{v \in V_h} \frac{(q, \nabla \cdot \boldsymbol{v})}{\|q\|_{L_0^2} \|\boldsymbol{v}\|_{\boldsymbol{H}^1}} \geq \gamma_h \geq \gamma_0 > 0.$$

In the context of Stokes, this condition is often called the Ladyzhenskaya–Babuska–Brezzi (LBB) condition, because Ladyzhenskaya first proved the continuous analog of the condition for the Stokes equations [19]; much of the challenge in solving Stokes lies in the selection of discrete spaces that satisfy this condition.

In [17], Boffi, Brezzi, and Fortin survey some choices for finite element discretizations to satisfy the LBB condition for the Stokes problem, among which are the MINI element, the Crouzeix–Raviart element, and the class of $Q_k - P_{k-1}$ elements. Generalized Hood–Taylor elements can be shown to satisfy the condition under certain regularity constraints on the mesh. (Each of these elements generalizes to three-dimensional spaces as well.)

It is worth noting that many stable elements use equal order approximation for pressure and velocity. For the mixed method, this leads to a suboptimal rate of convergence for pressure.

Cockburn et al. have applied the local discontinuous Galerkin (LDG) method [20] to the Stokes problem [21]; LDG derives its name from the local elimination of some variables (in the case of Stokes, the stresses)—by comparison with

standard DG methods, the global solve in LDG involves only about half as many unknowns, a significant savings. By means of carefully chosen numerical fluxes, the LDG method can enforce conservation laws weakly element by element, in a locally conservative way. The method also allows one to choose spaces for the pressure and velocity independently, so that they can use equal-order approximations, but they show that the convergence rate for pressure and stress will be of order one less than that for velocity. They numerically compare the efficiency of using lower-order approximations for pressure and stress with that of equal-order approximations, and conclude that in most cases the equal-order approximations are more efficient: although both choices yield the same *rate* of convergence, the lower-order approximation requires more degrees of freedom to achieve the same accuracy.

It is also worth emphasizing that finding these good spaces for the Stokes problem is *difficult* – this has been an area of ongoing research for decades. In this paper, we demonstrate that DPG allows the Stokes problem to be solved without any special effort – that is, the Stokes problem is approached and analyzed with exactly the same DPG-theoretical tools that we use for other linear problems, and we can use the same discrete spaces for velocity and pressure. In particular, we use equal-order spaces for velocity and pressure, and both pressure and velocity converge at the same rate, a contrast with LDG [21]. Indeed, one of our numerical experiments demonstrates not only that the method delivers the optimal convergence rate, but also that the method provides a solution close to the L^2 projection of the exact solution.

Our Stokes work began in collaboration with Pavel Bochev and Denis Ridzal in the summer of 2010 [8], when Roberts did an internship at Sandia. Bochev astutely suggested the Stokes problem as a good example problem for DPG. That summer, we were puzzled by the poor performance of DPG using what we herein refer to as the *naive* test space norm; the present analysis serves (among other things) to explain why the naive norm fails to achieve optimal convergence rates, in contrast to the choice to which our analysis leads us, which we here call the *adjoint graph* norm.

The structure of this paper is as follows. In Section 2, we present the general theory for the DPG method, and apply it to the Stokes problem. In Section 3 we detail some numerical experiments involving a manufactured solution and the lid-driven cavity flow problem. Section 4 concludes the paper, followed by an Appendix in which we show that the operator for the first-order Stokes system with homogeneous boundary conditions is bounded below.

2. Analysis

The purpose of this section is to present a general theory for the DPG method and linear PDEs and apply it to the Stokes problem. The presented theory summarizes results obtained in [9,22,23] for particular boundary-value problems and relates to the general theory for Friedrichs systems presented in [24]. Most of the technical results here are classical, so we adopt a somewhat informal style of presentation, making assumptions in the abstract setting as we need them.

We begin in Section 2.1 by establishing notation, definitions, and some basic properties of our functional setting. Then, in Section 2.2, we discuss, beginning with an abstract first-order linear operator, the strong and ultra-weak formulations of an arbitrary linear PDE, culminating in a proof of the well-posedness of the ultra-weak formulation. Along the way, we highlight some key assumptions that we make on the PDE, and verify those assumptions in the context of our Stokes formulation. Up to that point, we employ a continuous test space; in Section 2.3 we establish well-posedness in the context of the broken test spaces which are at the heart of DPG—these are what enable tractable determination of the optimal test functions. In Section 2.4 we discuss details of the boundary conditions and functional setting (including mechanisms for treating the pressure space) for the Stokes problem, expanding further on its satisfaction of our various assumptions. We summarize the results and the assumptions we have made along the way in Section 2.5.

2.1. Notation and definitions

Let Ω denote a bounded Lipschitz domain in $\mathbb{R}^n$, $n = 2$ or 3, with boundary $\Gamma = \partial\Omega$. We will employ the following energy spaces

$$H^1(\Omega) := \{u \in L^2(\Omega) : \nabla u \in \boldsymbol{L}^2(\Omega)\},$$
$$\boldsymbol{H}(\mathrm{div}, \Omega) := \{\boldsymbol{\sigma} \in \boldsymbol{L}^2(\Omega) : \mathrm{div}\,\boldsymbol{\sigma} \in L^2(\Omega)\},$$

with corresponding trace spaces on Γ:

$$H^{1/2}(\Gamma) := \{\hat{u} = u|_\Gamma,\ u \in H^1(\Omega)\},$$
$$H^{-1/2}(\Gamma) := \{\hat{\sigma}_n = (\boldsymbol{\sigma}\cdot\boldsymbol{n})|_\Gamma,\ \boldsymbol{\sigma} \in \boldsymbol{H}(\mathrm{div}, \Omega)\},$$

where $\boldsymbol{n}$ denotes the outward normal unit vector to boundary Γ. The definition of trace space $H^{1/2}(\Gamma)$ is classical but far from trivial, see e.g. [25, p. 96]. The assumption that the domain is Lipschitz is essential; domains with cracks require a special and non-classical treatment. We denote the trace operator by

$$\mathrm{tr} : H^1(\Omega) \ni u \to \mathrm{tr}\,u = \hat{u} = u|_\Gamma \in H^{1/2}(\Gamma).$$

The space $H^{-1/2}(\Gamma)$ is the topological dual of $H^{1/2}(\Gamma)$ and we similarly employ a second trace operator corresponding to it,

$$\mathrm{tr} : \boldsymbol{H}(\mathrm{div}, \Omega) \ni \boldsymbol{\sigma} \to \mathrm{tr}\,\boldsymbol{\sigma} = \hat{\sigma}_n = (\boldsymbol{\sigma}\cdot\boldsymbol{n})|_\Gamma \in H^{-1/2}(\Gamma),$$

which is usually defined by the *generalized Green Formula*; see e.g. [26, p. 61] or [27, p. 530]. Note that, unless otherwise stated, in this paper we use the same trace notation "tr" for functions in both $H^1(\Omega)$ and $\boldsymbol{H}(\mathrm{div}, \Omega)$.

We shall also use group variables consisting of multiple copies of functions from $H^1(\Omega)$, $\boldsymbol{H}(\mathrm{div}, \Omega)$, and $H^{1/2}(\Gamma)$ or distributions from $H^{-1/2}(\Gamma)$. We will employ boldface notation to distinguish the Cartesian product spaces from their scalar counterparts:

$$\begin{aligned}
\boldsymbol{H}^1(\Omega) &= H^1(\Omega) \times \cdots \times H^1(\Omega),\\
\boldsymbol{H}^{1/2}(\Gamma) &= H^{1/2}(\Gamma) \times \cdots \times H^{1/2}(\Gamma),\\
\boldsymbol{H}^{-1/2}(\Gamma) &= H^{-1/2}(\Gamma) \times \cdots \times H^{-1/2}(\Gamma),
\end{aligned}$$

etc. In the case of tensors, the definitions will be applied row-wise:

$$\boldsymbol{\sigma} = (\sigma_{ij}) \in \boldsymbol{H}(\mathbf{div}, \Omega) \Longleftrightarrow (\sigma_{i1}, \ldots, \sigma_{in}) \in \boldsymbol{H}(\mathrm{div}, \Omega), \quad i = 1, \ldots, n.$$

Broken energy spaces. Let Ω be partitioned into finite elements K such that

$$\overline{\Omega} = \bigcup_K \bar{K}, \quad K \text{ open},$$

with corresponding *skeleton* Γ_h and *interior skeleton* Γ_h^0,

$$\Gamma_h \coloneqq \bigcup_K \partial K \qquad \Gamma_h^0 \coloneqq \Gamma_h - \Gamma.$$

The usual regularity assumptions regarding the elements can be relaxed; the elements may be general polygons in 2D, or polyhedra[3] in 3D (with triangular and quadrilateral faces). Meshes may be *irregular*, i.e., may contain hanging nodes (see e.g. [28, p. 211]). In the *broken* energy spaces we simply mean standard energy spaces defined element-wise:

$$\begin{aligned}
H^1(\Omega_h) &\coloneqq \prod_K H^1(K),\\
\boldsymbol{H}(\mathrm{div}, \Omega_h) &\coloneqq \prod_K \boldsymbol{H}(\mathrm{div}, K).
\end{aligned}$$

With broken energy spaces, integration by parts is performed element-wise. For $\boldsymbol{\sigma} \in \boldsymbol{H}(\mathrm{div}, \Omega_h)$ and $v \in H^1(\Omega)$, we have

$$\begin{aligned}
(\mathrm{div}_h \boldsymbol{\sigma}, v)_{\Omega_h} &\coloneqq \sum_K (\mathrm{div}\, \boldsymbol{\sigma}, v)_K\\
&= \sum_K \left(-(\boldsymbol{\sigma}, \nabla v)_K + \langle \hat{\sigma}_n, \hat{v} \rangle_{\partial K} \right)\\
&= -(\boldsymbol{\sigma}, \nabla v) + \underbrace{\sum_K \langle \hat{\sigma}_n, \hat{v} \rangle_{\partial K}}_{=: \langle \hat{\sigma}_n, \hat{v} \rangle_{\Gamma_h}}.
\end{aligned}$$

Here $(\cdot, \cdot)$, $(\cdot, \cdot)_K$ denote the L^2 inner product over the whole domain and element K, respectively, and $\langle \cdot, \cdot \rangle_{\partial K}$ stands for the duality pairing between $H^{-1/2}(\partial K)$ and $H^{1/2}(\partial K)$.

This leads us naturally to the concept of the trace space over the skeleton Γ_h,

$$H^{1/2}(\Gamma_h) \coloneqq \left\{ \hat{v} = \{\hat{v}_K\} \in \prod_K H^{1/2}(\partial K) : \exists v \in H^1(\Omega) : v|_{\partial K} = \hat{v}_K \right\}.$$

This is not a trivial definition. First, by $v|_{\partial K}$ we mean the trace (for element K) of the restriction of v to K. Second, $H^{1/2}(\Gamma_h)$ is a *closed* subspace of $\prod_K H^{1/2}(\partial K)$. We take the trace spaces to be endowed with *minimum-energy extension norms*, given by

$$\|\hat{u}\|_{H^{1/2}(\partial K)} \coloneqq \inf_{\substack{u \in H^1(K)\\ u|_{\partial K} = \hat{u}}} \|u\|_{H^1(K)} \quad \text{and} \quad \|\widehat{\sigma_n}\|_{H^{-1/2}(\partial K)} \coloneqq \inf_{\substack{\boldsymbol{\sigma} \in \boldsymbol{H}(\mathrm{div},\, K)\\ (\boldsymbol{\sigma} \cdot \mathbf{n})|_{\partial K} = \widehat{\sigma_n}}} \|\boldsymbol{\sigma}\|_{\boldsymbol{H}(\mathrm{div},\, K)}.$$

To see that $H^{1/2}(\Gamma_h)$ is a closed subspace of the product space, let $\hat{u}^n = \{\hat{u}_K^n\} \in H^{1/2}(\Gamma_h)$ be a sequence of functions such that

$$\hat{u}^n \xrightarrow[\prod_K H^{1/2}(\partial K)]{} \hat{u} = \{\hat{u}_K\},$$

[3] Possibly curvilinear polyhedra.

where $\hat{u}$ is a member of the product space. We seek to show that there exists $u \in H^1(\Omega)$ such that $u|_{\partial K} = \hat{u}_K$ for each K, where again by $u|_{\partial K}$ we denote the element boundary trace of the restriction of u to element K. Let $u^n \in H^1(\Omega)$ be the minimum energy extension of $\hat{u}^n$, i.e. for each K, $\hat{u}^n_K = u^n|_{\partial K}$. By the definition of norms, $u^n|_K \overset{n\to\infty}{\longrightarrow} u_K$ in $H^1(K)$, for each element K. Now, the delicate question is whether we can claim that the union u of u_K is in $H^1(\Omega)$. We can show this by the definition of distributional derivatives. Consider a test function $\phi \in \mathcal{D}(\Omega)$.[4] For each n, the distributional derivative $\frac{\partial u^n}{\partial x_i}$ is defined by

$$\int_\Omega u^n \frac{\partial \phi}{\partial x_i} = -\int_\Omega \frac{\partial u^n}{\partial x_i}\phi$$

or, equivalently,

$$\sum_K \int_K u^n \frac{\partial \phi}{\partial x_i} = -\sum_K \int_K \frac{\partial u^n}{\partial x_i}\phi.$$

Passing to the limit $n \to \infty$, we have

$$\int_\Omega u \frac{\partial \phi}{\partial x_i} = -\sum_K \int_K \frac{\partial u_K}{\partial x_i}\phi,$$

which shows that the union of element-wise derivatives $\left\{\frac{\partial u_K}{\partial x_i}\right\}$ *is* the distributional derivative of u. Now, since $u_K \in H^1(K)$, $\frac{\partial u_K}{\partial x_i} \in L^2(K)$, so that the union $\left\{\frac{\partial u_K}{\partial x_i}\right\} \in L^2(\Omega)$. Consequently, $u \in H^1(\Omega)$.

Notice that we have not attempted to extend the classical definition of the trace space $H^{1/2}(\Gamma)$ for Lipschitz boundary Γ to a non-Lipschitz skeleton Γ_h.[5]

A similar construction holds for globally conforming $\boldsymbol{\sigma} \in \boldsymbol{H}(\mathrm{div}, \Omega)$ but broken $v \in H^1(\Omega_h)$:

$$\begin{aligned}(\boldsymbol{\sigma}, \nabla_h v)_{\Omega_h} &:= \sum_K (\boldsymbol{\sigma}, \nabla v)_K, \\ &= \sum_K \left(-(\mathrm{div}\,\boldsymbol{\sigma}, v)_K + \langle \hat{\sigma}_n, \hat{v}\rangle_{\partial K}\right), \\ &= -(\mathrm{div}\,\boldsymbol{\sigma}, v) + \underbrace{\sum_K \langle \hat{\sigma}_n, \hat{v}\rangle_{\partial K}}_{=:\langle \hat{\sigma}_n, \hat{v}\rangle_{\Gamma_h}}.\end{aligned}$$

In this case, we are led to the definition of the trace space $H^{-1/2}(\Gamma_h)$:

$$H^{-1/2}(\Gamma_h) := \left\{\hat{\sigma}_n = \{\hat{\sigma}_{Kn}\} \in \prod_K H^{-1/2}(\partial K) : \exists \boldsymbol{\sigma} \in \boldsymbol{H}(\mathrm{div}, \Omega) : \hat{\sigma}_{Kn} = (\boldsymbol{\sigma}\cdot\boldsymbol{n})|_{\partial K}\right\}.$$

We equip both trace spaces over the mesh skeleton with minimum energy extension norms

$$\|\hat{v}\|_{H^{1/2}(\Gamma_h)} := \inf_{\substack{u\in H^1(\Omega)\\ u|_{\Gamma_h}=\hat{v}}} \|u\|_{H^1(\Omega)} \quad \text{and}$$

$$\|\hat{\sigma}_n\|_{H^{-1/2}(\Gamma_h)} := \inf_{\substack{\boldsymbol{\sigma}\in\boldsymbol{H}(\mathrm{div},\Omega)\\ (\boldsymbol{\sigma}\cdot\boldsymbol{n})|_{\Gamma_h}=\hat{\sigma}_n}} \|\boldsymbol{\sigma}\|_{\boldsymbol{H}(\mathrm{div},\Omega)}.$$

We will also need the space of traces on the internal skeleton

$$\widetilde{H}^{1/2}(\Gamma_h) := \left\{\hat{v} = \{\hat{v}_K\} \in \prod_K H^{1/2}(\partial K) : \exists v \in H^1_0(\Omega) : v|_{\partial K} = \hat{v}_K\right\},$$

which we likewise equip with the minimum energy extension norm.

We have thus defined the term $\langle \hat{\sigma}_n, \hat{v}\rangle_{\Gamma_h}$ when one of the variables is a trace of a conforming function over the whole skeleton, and the other is the trace of a function from the broken energy space. For sufficiently regular functions, $\langle \hat{\sigma}_n, \hat{v}\rangle_{\Gamma_h}$ represents either the $L^2(\Gamma_h)$-product of the trace of a conforming $\boldsymbol{\sigma}$ and inter-element jumps of v, or the product of jumps in σ_n and the trace of a globally conforming v. This can be seen by switching from the summation over elements to the summation over element faces (edges in 2D).

[4] By $\mathcal{D}(\Omega)$ we understand the Schwartz space of test functions.

[5] The definition of a Lipschitz domain includes the assumption that the domain is on one side of its boundary; see [25, p. 89].

2.2. Strong and ultra-weak formulations

Integration by parts. Multiplying Eqs. (1.6a)–(1.6c) with test functions $\boldsymbol{v}, q, \boldsymbol{\tau}$, integrating by parts and summing up the equations, we obtain

$$\begin{aligned}(-\mathbf{div}\,(\boldsymbol{\sigma}-p\boldsymbol{I}),\boldsymbol{v})+(\operatorname{div}\boldsymbol{u},q)+(\boldsymbol{\sigma}-\nabla\boldsymbol{u},\boldsymbol{\tau}) &= (\boldsymbol{\sigma}-p\boldsymbol{I},\nabla\boldsymbol{v})+\langle(-\boldsymbol{\sigma}+p\boldsymbol{I})\boldsymbol{n},\boldsymbol{v}\rangle+(\boldsymbol{u},-\nabla q)+\langle\boldsymbol{u}\cdot\boldsymbol{n},q\rangle\\ &\quad+(\boldsymbol{\sigma},\boldsymbol{\tau})+(\boldsymbol{u},\mathbf{div}\,\boldsymbol{\tau})+\langle\boldsymbol{u},-\boldsymbol{\tau}\boldsymbol{n}\rangle\\ &= (\boldsymbol{u},\mathbf{div}\,(\boldsymbol{\tau}-q\boldsymbol{I}))+(p,-\operatorname{div}\boldsymbol{v})+(\boldsymbol{\sigma},\boldsymbol{\tau}+\nabla\boldsymbol{v})\\ &\quad+\langle(-\boldsymbol{\sigma}+p\boldsymbol{I})\boldsymbol{n},\boldsymbol{v}\rangle+\langle\boldsymbol{u},(-\boldsymbol{\tau}+q\boldsymbol{I})\boldsymbol{n}\rangle.\end{aligned}$$

It is convenient to think from the very beginning in more general terms, and use a more compact abstract notation. We therefore introduce group variables

$$u=(\boldsymbol{u},p,\boldsymbol{\sigma})\quad\text{and}$$
$$v=(\boldsymbol{v},q,\boldsymbol{\tau}),$$

as well as an operator A corresponding to the first order system and its formal adjoint A^*,

$$Au=(-\mathbf{div}\,(\boldsymbol{\sigma}-p\boldsymbol{I}),\operatorname{div}\boldsymbol{u},\boldsymbol{\sigma}-\nabla\boldsymbol{u}),$$
$$A^*v=(\mathbf{div}\,(\boldsymbol{\tau}-q\boldsymbol{I}),-\operatorname{div}\boldsymbol{v},\boldsymbol{\tau}+\nabla\boldsymbol{v}).$$

We can then rewrite the integration by parts formula in a compact form:

$$(Au,v)=(u,A^*v)+c(u,v). \tag{2.8}$$

Here $(\cdot,\cdot)$ denotes the $L^2(\Omega)$-inner product and $c(u,v)$ is the bilinear boundary term resulting from integration by parts. Obviously, the formula holds under appropriate regularity assumptions, e.g., $u, v \in C^1(\overline{\Omega})$, if all derivatives are understood in the classical sense.

If we assume $u, v \in L^2(\Omega)$ and interpret the derivatives in a distributional sense, we arrive naturally at the graph energy spaces

$$H_A(\Omega) \coloneqq \{u\in L^2(\Omega) : Au\in L^2(\Omega)\}\quad\text{and}$$
$$H_{A^*}(\Omega) \coloneqq \{u\in L^2(\Omega) : A^*u\in L^2(\Omega)\}.$$

The Stokes operator is not formally self-adjoint but the corresponding energy graph spaces are identical:

$$\begin{aligned}H_A(\Omega) &= \{(\boldsymbol{u},p,\boldsymbol{\sigma})\in\boldsymbol{L}^2(\Omega)\times L^2(\Omega)\times\boldsymbol{L}^2(\Omega) : \boldsymbol{\sigma}-p\boldsymbol{I}\in\boldsymbol{H}(\mathbf{div},\Omega),\boldsymbol{u}\in\boldsymbol{H}^1(\Omega)\};\\ H_A^*(\Omega) &= \{(\boldsymbol{v},q,\boldsymbol{\tau})\in\boldsymbol{L}^2(\Omega)\times L^2(\Omega)\times\boldsymbol{L}^2(\Omega) : \boldsymbol{\tau}-q\boldsymbol{I}\in\boldsymbol{H}(\mathbf{div},\Omega),\boldsymbol{v}\in\boldsymbol{H}^1(\Omega)\}.\end{aligned} \tag{2.9}$$

The graph spaces have trace operators

$$\begin{aligned}&\operatorname{tr}_A : H_A(\Omega)\ni(\boldsymbol{u},p,\boldsymbol{\sigma})\to(\underbrace{\widehat{(-\boldsymbol{\sigma}+p\boldsymbol{I})\boldsymbol{n}}}_{\hat{\boldsymbol{t}}},\hat{\boldsymbol{u}})\in\boldsymbol{H}^{-1/2}(\Gamma)\times\boldsymbol{H}^{1/2}(\Gamma)\quad\text{and}\\ &\operatorname{tr}_{A^*} : H_A(\Omega)\ni(\boldsymbol{v},q,\boldsymbol{\tau})\to(\underbrace{\widehat{(-\boldsymbol{\tau}+q\boldsymbol{I})\boldsymbol{n}}}_{\hat{\boldsymbol{r}}},\hat{\boldsymbol{v}})\in\boldsymbol{H}^{-1/2}(\Gamma)\times\boldsymbol{H}^{1/2}(\Gamma).\end{aligned} \tag{2.10}$$

Components $\hat{\boldsymbol{t}}$ and $\hat{\boldsymbol{r}}$ are defined by the trace operator for $\boldsymbol{H}(\mathbf{div},\Omega)$; components $\hat{\boldsymbol{u}}$ and $\hat{\boldsymbol{v}}$ are defined by the trace operator for $\boldsymbol{H}^1(\Omega)$.

On the abstract level, we assume the existence of two possibly distinct trace operators and trace spaces

$$\operatorname{tr}_A : H_A(\Omega)\twoheadrightarrow\hat{H}_A(\Gamma),\qquad u\to\hat{u}\quad\text{and}$$
$$\operatorname{tr}_{A^*} : H_{A^*}(\Omega)\twoheadrightarrow\hat{H}_{A^*}(\Gamma),\qquad v\to\hat{v}.$$

The double arrowheads indicate that the trace operators are surjective. For $u\in H_A(\Omega)$ in what follows, we will often use the notation $\hat{u}$ to denote $\operatorname{tr}_A u$; we will similarly use the notation $\hat{v}$ to denote $\operatorname{tr}_{A^*}v$ for $v\in H_{A^*}(\Omega)$. We equip the trace spaces with the minimum energy extension norms

$$\|\hat{u}\|_{\hat{H}_A(\Gamma)}=\inf_{\substack{u\in H_A(\Omega)\\ \operatorname{tr}_A u=\hat{u}}}\|u\|_{H_A(\Omega)}\quad\text{and}\quad\|\hat{v}\|_{\hat{H}_{A^*}(\Gamma)}=\inf_{\substack{v\in H_{A^*}(\Omega)\\ \operatorname{tr}_{A^*}v=\hat{v}}}\|v\|_{H_{A^*}(\Omega)}.$$

We can now extend the classical integration by parts formula (2.8) to a more general, distributional case:

$$(Au,v)=(u,A^*v)+c(\hat{u},\hat{v}), \tag{2.11}$$

with $u \in H_A(\Omega)$, $v \in H_{A^*}(\Omega)$, and the boundary bilinear form

$$c(\hat{u}, \hat{v}), \quad \hat{u} \in \hat{H}_A(\Gamma),\ \hat{v} \in \hat{H}_{A^*}(\Gamma)$$

defined on the trace spaces. Notice that the use of the minimum energy extension norm for traces is natural; the continuity constant for the form is one. For Stokes, we have:

$$c(\hat{u}, \hat{v}) = c((\hat{\boldsymbol{t}}, \hat{\boldsymbol{u}}), (\hat{\boldsymbol{r}}, \hat{\boldsymbol{v}})) = \langle \hat{\boldsymbol{u}}, \hat{\boldsymbol{r}} \rangle + \langle \hat{\boldsymbol{t}}, \hat{\boldsymbol{v}} \rangle.$$

Here and in what follows, $\langle \cdot, \cdot \rangle$ denotes the usual duality pairing between $\boldsymbol{H}^{1/2}(\Gamma)$ and $\boldsymbol{H}^{-1/2}(\Gamma)$ or, on the abstract level, between a Hilbert space and its dual. We may write the paired elements in either order.

The boundary form can be identified as a *duality pairing*,[6] i.e., a *definite* continuous bilinear (sesquilinear) form. Recall that form $c(\hat{u}, \hat{v})$ is definite if

$$\big(c(\hat{u}, \hat{v}) = 0\ \forall \hat{v}\big) \Longrightarrow \hat{u} = 0 \quad \text{and}$$
$$\big(c(\hat{u}, \hat{v}) = 0\ \forall \hat{u}\big) \Longrightarrow \hat{v} = 0.$$

Equivalently, the corresponding boundary operator C and its adjoint C'

$$C : \hat{H}_A(\Gamma) \to (\hat{H}_{A^*}(\Gamma))', \qquad \langle C\hat{u}, \hat{v} \rangle = c(\hat{u}, \hat{v})$$
$$C' : \hat{H}_{A^*}(\Gamma) \to (\hat{H}_A(\Gamma))', \qquad \langle \hat{u}, C'\hat{v} \rangle = c(\hat{u}, \hat{v})$$

are injective and, therefore, both are isomorphisms.[7]

Strong formulation with homogeneous boundary conditions. The boundary term for Stokes can be split into two parts according to the boundary conditions under consideration:

$$c(\hat{u}, \hat{v}) = c((\hat{\boldsymbol{t}}, \hat{\boldsymbol{u}}), (\hat{\boldsymbol{r}}, \hat{\boldsymbol{v}})) = \underbrace{\langle \hat{\boldsymbol{u}}, \hat{\boldsymbol{r}} \rangle}_{\langle C_1\hat{u}, \hat{v} \rangle} + \underbrace{\langle \hat{\boldsymbol{t}}, \hat{\boldsymbol{v}} \rangle}_{\langle C_2\hat{u}, \hat{v} \rangle};$$

i.e.,

$$C_1\hat{u} = C_1(\hat{\boldsymbol{t}}, \hat{\boldsymbol{u}}) = (0, \hat{\boldsymbol{u}}), \qquad C_2\hat{u} = C_2(\hat{\boldsymbol{t}}, \hat{\boldsymbol{u}}) = (\hat{\boldsymbol{t}}, 0).$$

We are interested in solving a non-homogeneous boundary-value problem,

$$\begin{cases} Au = f & \text{in } \Omega, \\ C_1\hat{u} = f_D & \text{on } \Gamma, \end{cases} \tag{2.12}$$

with $f \in L^2(\Omega)$ and $f_D \in \mathcal{R}(C_1)$.

In order to see the problem in its generality, we return now to our abstract setting and assume that the boundary operator C has been split into two operators C_1 and C_2,[8]

$$\begin{aligned} \langle C\hat{u}, \hat{v} \rangle &= \langle C_1\hat{u}, \hat{v} \rangle + \langle C_2\hat{u}, \hat{v} \rangle \\ &= \langle C_1\hat{u}, \hat{v} \rangle + \langle \hat{u}, C_2'\hat{v} \rangle; \end{aligned}$$

we also take C_1 and C_2 to be "reasonable", in the sense that both have closed range.

We begin with the case of homogeneous boundary conditions:

$$\begin{cases} Au = f & \text{in } \Omega, \\ C_1\hat{u} = 0 & \text{on } \Gamma. \end{cases} \tag{2.13}$$

Introducing the spaces

$$U := \{u \in H_A(\Omega) : C_1\hat{u} = 0\} \quad \text{and}$$
$$V := \{v \in H_{A^*}(\Omega) : C_2'\hat{v} = 0\},$$

we see that, if we restrict operators A and A^* to U and V, the boundary term vanishes. Recall now the abstract definition of the domain of the L^2-adjoint:

$$D(A^*) := \{v \in H_{A^*}(\Omega) : (Au, v) = (u, A^*v)\ \forall u \in D(A)\}$$

where, by assumption, $D(A) = U$.

The issue is not in the existence of the adjoint but in the characterization of its domain with operator C_2'. In order for V to coincide with the domain of the adjoint, we need to assume the condition:

$$\big(\langle \hat{u}, C_2'\hat{v} \rangle = 0\ \forall \hat{u} : C_1\hat{u} = 0\big) \Longrightarrow C_2'\hat{v} = 0. \tag{2.14}$$

---

6 Here we extend the definition of the usual duality pairing between a space and its dual.

7 $\mathcal{R}(C) = \mathcal{N}(C')^{\perp}$.

8 Here $\hat{u}$, $\hat{v}$ are generic elements of trace spaces.

Lemma 1. *Assume C has been split into C_1 and C_2 that satisfy condition (2.14). Each of the following conditions is then equivalent to (2.14).*

$$\begin{aligned} &\mathcal{N}(C_1)^\perp \cap \mathcal{R}(C_2') = \{0\}, \\ &\mathcal{N}(C_1)^\perp \cap \mathcal{N}(C_2)^\perp = \{0\}, \\ &X = \mathcal{N}(C_2) + \mathcal{N}(C_1). \quad \blacksquare \end{aligned} \tag{2.15}$$

Proof. Condition $(2.15)_1$ is just a reformulation of condition (2.14). The equivalence of $(2.15)_1$ and $(2.15)_2$ is implied by $\mathcal{R}(C_2') = \mathcal{N}(C_2)^\perp$. Finally, the equivalence of the last two conditions follows from the general algebraic property

$$(X_1 \cap X_2)^\perp = X_1^\perp + X_2^\perp,$$

which holds for any two closed subspaces X_1, X_2 of a Hilbert space X. $\blacksquare$

When $C : X \to Y$ is an isomorphism, the algebraic sum in the last condition can be upgraded to the direct sum:

$$X = \mathcal{N}(C_2) \oplus \mathcal{N}(C_1).$$

Indeed, $\mathcal{N}(C_2) \cap \mathcal{N}(C_1) \subset \mathcal{N}(C) = \{0\}$.

Condition (2.14) thus decomposes the trace space $\hat{H}_A(\Gamma)$ into the direct sum of the null spaces of operators C_2 and C_1;

$$\hat{H}_A(\Gamma) = \hat{H}_A^1(\Gamma) \oplus \hat{H}_A^2(\Gamma), \tag{2.16}$$

where $\hat{H}_A^1(\Gamma) := \mathcal{N}(C_2)$ and $\hat{H}_A^2(\Gamma) := \mathcal{N}(C_1)$. In other words, for each $\hat{u} \in \hat{H}_A(\Gamma)$, there exist unique $\hat{u}_1 \in \hat{H}_A^1(\Gamma)$ and $\hat{u}_2 \in \hat{H}_A^2(\Gamma)$ such that

$$\hat{u} = \hat{u}_1 + \hat{u}_2, \tag{2.17}$$

which is analogous to the condition introduced by Friedrichs [29] for his boundary operator M, subsequently generalized in [30], and first used in the DPG context in [11]. For the Stokes problem under consideration the decomposition is very simple:

$$(\hat{\boldsymbol{t}}, \hat{\boldsymbol{u}}) = (0, \hat{\boldsymbol{u}}) + (\hat{\boldsymbol{t}}, 0).$$

Having reduced the problem with homogeneous boundary conditions to the classical theory of L^2-adjoint operators, we now recall that the following conditions are equivalent to each other [31].

i. $A|_U$ has a closed range.
ii. $A^*|_V$ has a closed range.
iii. $\|Au\| \geq \gamma \|u\| \ \forall u \in \mathcal{N}(A)^\perp$.
iv. $\|A^* v\| \geq \gamma \|v\| \ \forall v \in \mathcal{N}(A^*)^\perp$.

Note that (maximal) constant γ is the same for both operators.

We now assume at the abstract level that the equivalent conditions above are satisfied. The homogeneous problem (2.13) and its adjoint counterpart are thus well-posed. More precisely, for each data function f which is L^2-orthogonal to the null space of the adjoint operator, a solution exists, is unique in the orthogonal complement of the null space of the operator (equivalently, in the corresponding quotient space), and depends continuously on f. The inverse of the maximal constant γ can be identified as the norm of the solution operator from $\mathcal{R}(A)$ into $\mathcal{N}(A)^\perp$ (equal to the norm of the solution operator for the adjoint, from $\mathcal{R}(A^*)$ into $\mathcal{N}(A^*)^\perp$).

For the Stokes problem, with a little abuse of notation, we have

$$C_1 \hat{u} = \hat{\boldsymbol{u}} \quad \text{and} \quad C_2' \hat{v} = \hat{\boldsymbol{v}}.$$

Condition (2.14) is easily verified. We have $U = V$,

$$\begin{aligned} U &= \{(\boldsymbol{u}, p, \boldsymbol{\sigma}) \in \boldsymbol{L}^2(\Omega) \times L^2(\Omega) \times \boldsymbol{L}^2(\Omega) : \boldsymbol{\sigma} - p\boldsymbol{I} \in \boldsymbol{H}(\mathbf{div}, \Omega), \boldsymbol{u} \in \boldsymbol{H}_0^1(\Omega)\} \\ V &= \{(\boldsymbol{v}, q, \boldsymbol{\tau}) \in \boldsymbol{L}^2(\Omega) \times L^2(\Omega) \times \boldsymbol{L}^2(\Omega) : \boldsymbol{\tau} - q\boldsymbol{I} \in \boldsymbol{H}(\mathbf{div}, \Omega), \boldsymbol{v} \in \boldsymbol{H}_0^1(\Omega)\}. \end{aligned} \tag{2.18}$$

Both A and A^* have non-trivial null space consisting of constant pressures. To ensure uniqueness, we restrict ourselves to pressures p and q with zero average;

$$p, q \in L_0^2 := \left\{ q \in L^2(\Omega) : \int_\Omega q = 0 \right\}.$$

The proof that A and A^* are bounded below follows from the classical inf–sup condition for the Stokes problem; for the reader's convenience we reproduce the standard reasoning in the Appendix.

Strong formulation with non-homogeneous boundary conditions. We are now ready to tackle the case with non-homogeneous boundary conditions. We have

$$(Au, v) - \langle C_1\hat{u}, \hat{v}\rangle = (u, A^*v) + \langle \hat{u}, C_2'\hat{v}\rangle \quad u \in H_A(\Omega),\ v \in H_{A^*}(\Omega).$$

We are interested in the operators

$$\begin{aligned} &H_A(\Omega) \ni u \to (Au, C_1\hat{u}) \in L^2(\Omega) \times (\hat{H}_{A^*}(\Gamma))' \quad \text{and} \\ &H_{A^*}(\Omega) \ni v \to (A^*v, C_2'\hat{v}) \in L^2(\Omega) \times (\hat{H}_A(\Gamma))'. \end{aligned} \tag{2.19}$$

We have the following classical result.

Theorem 1. *Assume that data $f \in L^2(\Omega)$ and $f_D \in \mathcal{R}(C_1)$ satisfy the compatibility condition*

$$(f, v) - \langle f_D, \hat{v}\rangle = 0 \quad \forall v : A^*v = 0, \qquad C_2'\hat{v} = 0.$$

Problem (2.12) has a unique solution u in $\mathcal{N}(A)^\perp$ that depends continuously upon the data; i.e., there exists a constant $\widetilde{\gamma} > 0$, independent of the data, such that

$$\widetilde{\gamma}\|u\|_{H_A(\Omega)} \le \left(\|f\|^2 + \|f_D\|^2\right)^{1/2}.$$

The analogous result holds for the adjoint operator (A^*, C_2'). ■

Proof. The usual way to tackle the problem with non-homogeneous boundary conditions is to reduce it to the case of homogeneous conditions using a particular solution satisfying the non-homogeneous conditions. We present an alternate approach. We introduce a bilinear form

$$b(u, (w_1, \hat{w}_2)) = (Au, w_1) - \langle C_1\hat{u}, \hat{w}_2\rangle, \quad u \in H_A(\Omega),\ w_1 \in L^2(\Omega),\ \hat{w}_2 \in W_2,$$

where W_2 is given by

$$W_2 = \{\hat{w}_2 \in \hat{H}_{A^*}(\Gamma) : C_2'\hat{w}_2 = 0\}.$$

We then consider the corresponding variational problem,

$$b(u, (w_1, \hat{w}_2)) = (f, w_1) - \langle f_D,\ \hat{w}_2\rangle \quad \forall w_1 \in L^2(\Omega),\ \hat{w}_2 \in W_2. \tag{2.20}$$

We begin by determining the null space of the conjugate operator:

$$\{(w_1, \hat{w}_2) \in L^2(\Omega) \times W_2 : b(u, (w_1, \hat{w}_2)) = 0\ \forall u \in H_A(\Omega)\}.$$

Consider $(w_1, \hat{w}_2)$ in the null space. Selecting $u \in \mathcal{D}(\Omega)$, we see that $A^*w_1 = 0$. Therefore, w_1 lies in the energy space $H_{A^*}(\Omega)$, and we may integrate by parts to obtain

$$\begin{aligned} 0 = b(u, (w_1, \hat{w}_2)) &= (Au, w_1) - \langle C_1\hat{u}, \hat{w}_2\rangle \\ &= (u, \underbrace{A^*w_1}_{=0}) + \langle C_1\hat{u}, \hat{w}_1 - \hat{w}_2\rangle + \langle \hat{u}, C_2'\hat{w}_1\rangle. \end{aligned}$$

Due to the arbitrariness of trace $\hat{u}$, $C_2'\hat{w}_1 = 0$ and $\hat{w}_1 = \hat{w}_2$. This establishes the necessary condition for the existence of solutions. We now proceed to prove the inf–sup condition. Since the test space is Hilbert, we have:

$$\sup_{(w_1, \hat{w}_2)} \frac{|(Au, w_1) - \langle C_1\hat{u}, \hat{w}_2\rangle|}{(\|w_1\|^2 + \|\hat{w}_2\|^2_{\hat{H}_{A^*}(\Gamma)})^{1/2}} = (\|Au\|^2 + \|C_1\hat{u}\|^2_{W_2'})^{1/2} \ge (\|Au\|^2 + \beta\|C_1\hat{u}\|^2_{(\hat{H}^*_A(\Gamma))'})^{1/2}.$$

where β depends upon the angle between the spaces $\mathcal{N}(C_1')$ and $\mathcal{N}(C_2')$.

Let $u_{C_1} \in H_A(\Omega)$ be such that $C_1\,\mathrm{tr}_A\, u_{C_1} = C_1\hat{u}$ and

$$u_{C_1} = \arg\min_z \|Az\| \quad \text{or, equivalently,} \quad (Au_{C_1}, Au_0) = 0 \quad \forall u_0 \in U.$$

Splitting u into u_{C_1} and $u_0 := u - u_{C_1}$, we have:

$$\|Au\|^2 = \|Au_{C_1}\|^2 + \|Au_0\|^2.$$

The boundedness below of $A|_U$ implies that

$$\|u_0\| \le \frac{1}{\gamma}\|Au_0\| \le \|Au\|.$$

It remains to show that we also control $\|u_{C_1}\|$. Recall the splitting defined in (2.17):

$$\hat{u} = \hat{u}_1 + \hat{u}_2, \qquad C_2\hat{u}_1 = 0, \qquad C_1\hat{u}_2 = 0.$$

Consider the minimum energy extension $\widetilde{u_1}$ of $\hat{u}_1$. We have

$$\|\widetilde{u_1}\|_{H_A(\Omega)} = \|\hat{u}_1\|_{\hat{H}_A(\Gamma)} \leq \frac{1}{\delta}\|C\hat{u}_1\|_{(\hat{H}_{A^*(\Gamma)})'} = \frac{1}{\delta}\|C_1\hat{u}\|_{(\hat{H}_{A^*(\Gamma)})'},$$

where $1/\delta$ is the norm of operator C^{-1}. We now have

$$\begin{aligned}
\|u_{C_1}\| &\leq \|\widetilde{u_1}\| + \|u_{C_1} - \widetilde{u_1}\| \\
&\leq \frac{1}{\delta}\|C_1\hat{u}\|_{(\hat{H}_{A^*(\Gamma)})'} + \frac{1}{\gamma}\|A(u_{C_1} - \widetilde{u_1})\| \\
&\leq \frac{1}{\delta}\|C_1\hat{u}\|_{(\hat{H}_{A^*(\Gamma)})'} + \frac{1}{\gamma}\|Au_{C_1}\| + \frac{1}{\gamma}\|\widetilde{u_1}\|_{H_A(\Omega)} \\
&= \frac{1}{\delta}\|C_1\hat{u}\|_{(\hat{H}_{A^*(\Gamma)})'} + \frac{1}{\gamma}\|Au_{C_1}\| + \frac{1}{\gamma}\|\hat{u}_1\|_{\hat{H}_A(\Gamma)} \\
&\leq \frac{1}{\delta}\left(1 + \frac{1}{\gamma}\right)\|C_1\hat{u}\|_{(\hat{H}_{A^*(\Gamma)})'} + \frac{1}{\gamma}\|Au_{C_1}\|,
\end{aligned}$$

which finishes the proof. Note that the inf–sup constant can be expressed in terms of γ, β, and δ. ■

Strong formulation with non-homogeneous boundary conditions for the Stokes problem. The ranges of operators C_1 and C_2' coincide exactly with $\{\mathbf{0}\} \times \boldsymbol{H}^{1/2}(\boldsymbol{\Gamma})$. The strong formulation for the non-homogeneous Stokes problem is well-posed, provided the data g and $\boldsymbol{u}_D$ satisfy the compatibility condition

$$\int_\Omega g = \int_\Gamma \boldsymbol{u}_D \cdot \boldsymbol{n}.$$

The analogous conclusion holds for the adjoint operator.

Ultra-weak (variational) formulation. We are now ready to formulate the *ultra-weak variational formulation* for problem (2.12). The steps are as follows.

1. Integrate by parts:
$$(u, A^*v) + \langle C\hat{u}, \hat{v}\rangle = (f, v).$$
2. Split the boundary operator C into C_1 and C_2 according to the decomposition in (2.16):
$$(u, A^*v) + \langle C_1\hat{u}_1, \hat{v}\rangle + \langle C_2\hat{u}_2, \hat{v}\rangle = (f, v).$$
3. Apply the boundary conditions, moving the known term $C_1\hat{u}_1 = f_D$ to the right-hand side:
$$(u, A^*v) + \langle \hat{u}_2, C_2'\hat{v}\rangle = (f, v) - \langle f_D, \hat{v}\rangle.$$
4. Extend the domain of u to $L^2(\Omega)$ and define $\hat{u}_2$ as an independent unknown.[9] The problem then becomes
$$\begin{cases} \text{Find } u \in L^2(\Omega),\ \hat{u}_2 \in \hat{H}_A^2(\Gamma) \text{ such that} \\ (u, A^*v) + \langle \hat{u}_2, C_2'\hat{v}\rangle = (f, v) - \langle f_D, \hat{v}\rangle \quad \forall v \in H_{A^*}(\Omega). \end{cases} \tag{2.21}$$

The bilinear form

$$b((u, \hat{u}_2), v) := (u, A^*v) + \langle \hat{u}_2, C_2'\hat{v}\rangle = (u, A^*v) + c(\hat{u}_2, \hat{v}) \tag{2.22}$$

generates two associated operators B and B', where

$$b((u, \hat{u}_2), v) = \langle B(u, \hat{u}_2), v\rangle = \langle (u, \hat{u}_2), B'v\rangle.$$

Operator B' corresponds to the strong setting for the adjoint A^* with non-homogeneous boundary conditions;

$$B'v = (A^*v, C_2'\hat{v}) \in L^2(\Omega) \times (\hat{H}_A(\Gamma))'.$$

In order to determine the null space of operator B, assume that

$$b((u, \hat{u}_2), v) = 0 \quad \forall v \in H_{A^*}(\Omega).$$

Testing first with $v \in \mathcal{D}(\Omega)$, we deduce that $Au = 0$. Integrating the first term by parts, and testing with arbitrary v, we learn that the null space of operator B consists of $(u, \hat{u}_2)$ such that $\hat{u}_2 = u$ on Γ and $C_1u = 0$.

[9] Watch out for the notation. With $u \in L^2(\Omega)$, $\hat{u}$ no longer denotes the trace of u but *an independent unknown*.

Theorem 2. *Problem (2.21) is well-posed. In particular, for each $f \in L^2(\Omega)$ and $f_D \in \mathcal{R}(C_1)$ that satisfy the compatibility condition*

$$(f, v) - \langle f_D, \hat{v}\rangle = 0 \quad \forall v \in \mathcal{N}(A^*|_V), \tag{2.23}$$

a solution of (2.21) exists and it is unique up to $u \in \mathcal{N}(A|_U)$ and corresponding $\hat{w}_2 \in \hat{H}^2_A(\Gamma)$ such that $\hat{w}_2 = \hat{u}_2$, where $\hat{u}_2$ is the component of trace $\hat{u}$ of u in $\hat{H}^2_A(\Gamma)$.

The inf–sup constant for bilinear form (2.22) is equal to the inf–sup constant of the adjoint operator (A^*, C_2') from Theorem 1. ■

Proof. We observe that the conjugate B' of operator B corresponding to the bilinear form (2.22) coincides with the strong form of operator (A^*, C_2'). The result is then a direct consequence of Theorem 1. ■

Ultra-weak formulation for the Stokes problem. The Stokes formulation is now just a matter of interpretation. The solution consists of $u = (\boldsymbol{u}, p, \boldsymbol{\sigma})$ and unknown traction

$$\hat{\boldsymbol{t}} = (-\boldsymbol{\sigma} + p\boldsymbol{I})\boldsymbol{n}. \tag{2.24}$$

Remember that only for a sufficiently regular[10] solution u will $\hat{\boldsymbol{t}}$ coincide with the trace $(-\boldsymbol{\sigma} + p\boldsymbol{I})\boldsymbol{n}$. In the ultra-weak formulation, the traction $\hat{\boldsymbol{t}}$ appears as an *independent* unknown. With a homogeneous incompressibility constraint, the ultra-weak variational problem reads as follows.

$$\begin{cases} \text{Find } \boldsymbol{u} \in \boldsymbol{L}^2(\Omega),\ p \in L^2(\Omega),\ \boldsymbol{\sigma} \in \boldsymbol{L}^2(\Omega),\ \hat{\boldsymbol{t}} \in H^{-1/2}(\Gamma) \text{ such that} \\ (\boldsymbol{u}, \mathbf{div}\,(\boldsymbol{\tau} - q\boldsymbol{I})) + (p, -\mathrm{div}\, q) + (\boldsymbol{\sigma}, \boldsymbol{\tau} + \nabla \boldsymbol{v}) + \langle \hat{\boldsymbol{t}}, \boldsymbol{v}\rangle = (\boldsymbol{f}, \boldsymbol{v}) - \langle \boldsymbol{u}_D, (-\boldsymbol{\tau} + q\boldsymbol{I})\boldsymbol{n}\rangle \\ \quad \forall (\boldsymbol{v}, q, \boldsymbol{\tau}) \text{ such that } \boldsymbol{\tau} - q\boldsymbol{I} \in \boldsymbol{H}(\mathbf{div}, \Omega), \boldsymbol{v} \in \boldsymbol{H}^1(\Omega). \end{cases}$$

For Stokes,[11]

$$f \overset{'}{=} (\boldsymbol{f}, 0, \boldsymbol{0}), \qquad f_D \overset{'}{=} (\boldsymbol{0}, \boldsymbol{u}_0).$$

The null space of adjoint $A^*|_V$,

$$\mathcal{N}(A^*|_V) = \{(\boldsymbol{v}, q, \boldsymbol{\tau}) = (\boldsymbol{0}, q_0, \boldsymbol{0})\ q_0 \in \mathbb{R}\},$$

and the abstract compatibility condition on the load reduces to:

$$(f, v) - \langle f_D, \hat{v}\rangle = 0 - \int_\Gamma (\boldsymbol{u}_D \cdot \boldsymbol{n}) q_0 = 0.$$

In other words, the problem is well-posed if

$$\int_\Gamma \boldsymbol{u}_D \cdot \boldsymbol{n} = 0. \tag{2.25}$$

The null space of $A|_U$ consists of constant pressures,

$$\mathcal{N}(A|_U) = \{(\boldsymbol{u}, p, \boldsymbol{\sigma}) = (\boldsymbol{0}, p_0, \boldsymbol{0})\ p_0 \in \mathbb{R}\},$$

and, for $u \in \mathcal{N}(A|_U)$, the corresponding trace reduces to

$$\hat{u} = (\underbrace{p_0\boldsymbol{n}}_{\hat{u}_2 = \hat{w}_2}, \boldsymbol{0}).$$

The solution is thus determined up to a constant pressure p_0 and corresponding constant traction $\hat{\boldsymbol{t}}_0 = p_0\boldsymbol{n}$.

Notice that there are no boundary conditions imposed on the test functions. This is important from a practical point of view.

Remark 1 (*Choice of Unknowns on the Boundary*)**.** Returning to the abstract setting, notice that by construction there is a one-to-one correspondence between traces $\hat{u}_1, \hat{u}_2$ and the values of the corresponding boundary operators $C_1\hat{u}_1, C_2\hat{u}_2$. If we can identify the range of operator C_2 explicitly, we may solve for $C_2\hat{u}_2$ in place of $\hat{u}_2$. For the discussed Stokes problem, the difference between the two formulations is trivial. In the first case we solve for $(0, \hat{\boldsymbol{t}})$, in the second one, for $\hat{\boldsymbol{t}}$. The difference becomes apparent for less trivial boundary conditions, e.g., impedance conditions in acoustics or various boundary conditions for hyperbolic systems. ■

[10] That is, $u \in H_A(\Omega)$.

[11] We are using the $\overset{'}{=}$ symbol for equality in metalanguage expressing correspondence between the abstract theory and Stokes.

Remark 2 (*Strong Versus Weak Imposition of Boundary Conditions*)**.** In the classical variational formulation for second order elliptic PDEs, we distinguish between *strong* (Dirichlet) boundary conditions and weak (Neumann) conditions. Dirichlet conditions are accounted for by determining a finite-energy lift of the boundary data, and looking for a solution to the problem with homogeneous boundary conditions and the *generalized load vector* including the action of the bilinear form on the lift. In principle, we can work with any lift of the Dirichlet data. The discrete solution, being the sum of the lift and the discrete solution of the homogeneous problem, then depends upon the lift. With such an approach, degrees of freedom corresponding to the Dirichlet data do not enter the computations.

In practice, we prefer to project (interpolate) the Dirichlet data first onto the trace of the finite element space and only then lift it with finite element shape functions. The solution depends upon the interpolation procedure but the dependence upon the lift is eliminated as both the lift and the solution to the homogeneous problem live in the finite element space. The second approach is preferred for many reasons, including the fact that it simplifies graphical postprocessing and error analysis.

By contrast to the situation with Dirichlet conditions, Neumann conditions simply contribute to the load vector. We call the imposition of Dirichlet conditions *strong*, referring to the fact that the error in satisfying the Dirichlet data depends only upon the interpolation procedure. In particular, if the Dirichlet data live in the finite element space, the error is zero—the boundary conditions are satisfied exactly (though in itself this affords no guarantee of the overall quality of the solution). The Neumann conditions are satisfied only in the limit as the solution converges; hence, we call the imposition of Neumann data *weak*.

A possibly subtle point: in the ultra-weak variational formulation, the boundary conditions are satisfied in the strong sense. In formulation (2.21), the implicit choice of unknowns on the boundary is $C_1\hat{u}_1$ and $\hat{u}_2$, and the first unknown is determined by the BC. If we decide to work with $\hat{u}_1$ in place of $C_1\hat{u}_1$, we need to start by finding a lift $\hat{u}_0$ of the BC to the whole trace space,

$$C_1\hat{u}_0 = f_D.$$

Notice that the lift may have a non-zero $\hat{H}^2_A$-component but the final trace will be equal to the sum of the lift and an unknown component $\hat{u}_2 \in \hat{H}^2_A$,

$$\hat{u} = \hat{u}_0 + \hat{u}_2.$$

The term $\langle f_D, \hat{v}\rangle$ on the right-hand side of (2.22) is then simply replaced with $c(\hat{u}_0, \hat{v})$. The rest of the formulation remains unchanged. The difference between the two formulations will become clearer in the context of discontinuous test functions discussed next.

For the discussed Stokes problem, the C_1, C_2 operators are very simple: $C_1(\hat{\boldsymbol{u}}, \hat{\boldsymbol{t}}) = \hat{\boldsymbol{u}}$, $C_2(\hat{\boldsymbol{u}}, \hat{\boldsymbol{t}}) = \hat{\boldsymbol{t}}$, and the two approaches are hardly distinguishable from each other.

Finally, as in classical finite element methods, if $\boldsymbol{u}_D$ lies outside the discrete (trace) space, we replace it with its discrete interpolant. ■

2.3. DPG formulation

The essence of the DPG formulation lies in extending the concept of the ultra-weak variational formulation to broken test spaces. We begin by partitioning domain Ω into finite elements K and applying integration by parts to a single element:

$$(Au, v)_K = (u, A^*v)_K + c_{\partial K}(\hat{u}, \hat{v}) \quad u \in H_A(K),\ v \in H_{A^*}(K). \tag{2.26}$$

Next, we sum up over all elements to obtain

$$\underbrace{\sum_K (Au, v)_K}_{=(Au,v)} = \underbrace{\sum_K (u, A^*v)_K}_{=:(u,A_h^*v)_h} + \underbrace{\sum_K c_{\partial K}(\hat{u}, \hat{v})}_{=:c_h(\hat{u},\hat{v})} \quad u \in H_A(\Omega),\ v \in H_{A^*}(\Omega_h). \tag{2.27}$$

Above we have kept u globally conforming but v comes from the broken Sobolev space:

$$H_{A^*}(\Omega_h) := \{v \in L^2(\Omega) : A^*v|_K \in L^2(K)\ \forall K\}. \tag{2.28}$$

The subscript h is intended as a reminder that the formal adjoint operator is to be understood element-wise. The boundary term extends now to the whole skeleton $\Gamma_h = \cup_K \partial K$. For the internal skeleton $\Gamma_h^0 = \Gamma_h - \Gamma$, this represents the action of traces $\hat{u}$ on the jumps of traces $\hat{v}$. Just as we did with spaces $H^{1/2}(\Gamma_h), H^{-1/2}(\Gamma_h)$, here we introduce a general, abstract space of traces on the skeleton,

$$\hat{H}_A(\Gamma_h) := \left\{\hat{u} = \{\hat{u}_K\} \in \prod_K \hat{H}_A(\partial K) : \exists u \in H_A(\Omega) : \mathrm{tr}_A u|_K = \hat{u}_K\right\}, \tag{2.29}$$

and the corresponding subspace of traces vanishing on $\Gamma = \partial\Omega$,

$$\widehat{\widetilde{H}}_A(\Gamma_h) := \left\{ \hat{u} = \{\hat{u}_K\} \in \prod_K \hat{H}_A(\partial K) : \exists u \in \widetilde{H}_A(\Omega) : \mathrm{tr}_A u|_K = \hat{u}_K \right\}, \tag{2.30}$$

where

$$\widetilde{H}_A(\Omega) = \{u \in H_A(\Omega) : \mathrm{tr}\, u = 0 \text{ on } \Gamma\}. \tag{2.31}$$

As usual, we equip the trace space with the minimum energy extension norm.[12]

Any function $u \in H_A(\Omega)$ can be decomposed into an extension of its trace on Γ and a component vanishing on Γ:

$$u = E(\mathrm{tr}\, u) + \widetilde{u}, \quad \widetilde{u} \in \widetilde{H}_A(\Omega). \tag{2.32}$$

If the extension $E(\mathrm{tr}\, u)$ is the minimum-energy extension, the decomposition above is H_A-orthogonal. There is a corresponding decomposition for traces $\hat{u} \in \hat{H}_A(\Gamma_h)$:

$$\hat{u} = \hat{E}\hat{u}_0 + \widehat{\widetilde{u}}, \quad \widehat{\widetilde{u}} \in \widehat{\widetilde{H}}_A(\Gamma_h). \tag{2.33}$$

Here $\hat{u}_0 \in \hat{H}_A(\Gamma)$ is the restriction[13] of $\hat{u}$ to Γ and $\hat{E}\hat{u}_0 \in \hat{H}_A(\Gamma_h)$ is any extension of $\hat{u}_0$ back to the whole skeleton Γ_h. Again, if we use the minimum-energy extension, the decomposition is $\hat{H}_A(\Gamma_h)$-orthogonal. We then have

$$\hat{H}_A(\Gamma_h) = \hat{E}\hat{H}_A(\Gamma) \oplus \widehat{\widetilde{H}}_A(\Gamma_h). \tag{2.34}$$

By construction, we have a generalization of the trace operator to the whole skeleton,

$$\mathrm{tr} : H_A(\Omega) \twoheadrightarrow \hat{H}_A(\Gamma_h). \tag{2.35}$$

The skeleton term $c_h(\hat{u}, \hat{v}) = \sum_K c_{\partial K}(\hat{u}, \hat{v})$ is well-defined for $\hat{u} \in \hat{H}_A(\Gamma_h)$ and $\hat{v} = \{\hat{v}_K\} \in \prod_K H_{A^*}(\partial K)$. We also have the condition:

$$(c_h(\widehat{\widetilde{u}}, \hat{v}) = 0 \,\forall\, \widehat{\widetilde{u}} \in \widehat{\widetilde{H}}_A(\Gamma_h)) \Longleftrightarrow v \in H_{A^*}(\Omega). \tag{2.36}$$

Indeed, if we restrict ourselves to a globally conforming test function, the skeleton term reduces to a term involving only the domain boundary Γ, where the trace $\widehat{\widetilde{u}}$ vanishes. The converse follows from the definition of distributional derivatives. Indeed, for any test function $\phi \in \mathcal{D}(\Omega)$, we have

$$c_h(\mathrm{tr}\, \phi, \hat{v}) = (A\phi, v) - (\phi, A_h^* v)_h = 0, \tag{2.37}$$

which proves that the union of element-wise values $A_h^* v$ (which lies in $L^2(\Omega)$) is equal to $A^* v$ in the sense of distributions.

We now use the decomposition of traces (2.34) to set up the boundary operators. Recall that condition (2.14) established a decomposition of the trace space $\hat{H}_A(\Gamma)$ into a direct sum of the null spaces of operators C_2 and C_1,

$$\hat{H}_A(\Gamma) = \hat{H}_A^1(\Gamma) \oplus \hat{H}_A^2(\Gamma), \qquad \hat{u} = \hat{u}_1 + \hat{u}_2. \tag{2.38}$$

The first term is known from the boundary condition; the second remains as an additional unknown. We have

$$\begin{aligned} c_h(\hat{u}, \hat{v}) &= c_h(\hat{E}\hat{u}_0, \hat{v}) + c_h(\widehat{\widetilde{u}}, \hat{v}) \\ &= c_h(\hat{E}\hat{u}_0^1, \hat{v}) + c_h(\hat{E}\hat{u}_0^2, \hat{v}) + c_h(\widehat{\widetilde{u}}, \hat{v}). \end{aligned} \tag{2.39}$$

For conforming test functions $\hat{v} \in \hat{H}_{A^*}(\Gamma_h)$, the bilinear form on the skeleton reduces to the bilinear form on the domain boundary,

$$c_h(\hat{u}, \hat{v}) = c(\hat{u}, \hat{v}) = c(\hat{u}_0^1, \hat{v}) + c(\hat{u}_0^2, \hat{v}) = \langle f_D, \hat{v}\rangle + c(\hat{u}_0^2, \hat{v}).$$

In particular, this is independent of the choice of lift $\hat{E}$. If we identify $\hat{u}_1$ as the unknown, we need to find a trace lift of the BC data f_D,

$$C_1\hat{u}_0 = f_D,$$

[12] For Stokes, tr_A and tr_{A^*} are composed of the H^1 and $H(\mathrm{div})$ traces, so the spaces $\hat{H}_A(\Gamma_h)$ and $\hat{H}_{A^*}(\Gamma_h)$ are complete. We are not claiming any results on traces for the general, abstract graph energy spaces. If we did have them, though, the proof of completeness would have proceeded along the same lines as for the H^1 and $H(\mathrm{div})$ cases.

[13] Note that the restriction is well-defined. For $\hat{u} \in \hat{H}_A(\Gamma_h)$, there exists an extension $u \in H_A(\Omega)$ which has a trace $\hat{u}_0$ on Γ. This trace is independent of the extension and, therefore, it can be identified as a trace of $\hat{u}$ on Γ.

move the term with the lift to the right-hand side, and solve for the unknown component $\hat{u}_2$ of the trace on Γ. The final formulation is as follows.

$$\begin{cases} u \in L^2(\Omega),\, \hat{u} \in \hat{E}\hat{H}^2_A(\Gamma) \oplus \widetilde{\widehat{H}}_A(\Gamma_h) \\ (u, A_h^* v)_h + c_h(\hat{u}, v) = (f, v) - c_h(\hat{E}\hat{u}_0, \hat{v}) \quad \forall v \in H_{A^*}(\Omega_h). \end{cases} \tag{2.40}$$

However, if we decide to work with $C_1\hat{u} = f_D$ directly, we need to replace the first term on the right-hand side of (2.39) with an extension of known BC data $\langle f_D, \hat{v}\rangle$ to discontinuous test functions. The term $c_h(\hat{E}\hat{u}_0, \hat{v})$ is one such extension.

The final abstract DPG formulation[14] is then as follows:

$$\begin{cases} u \in L^2(\Omega),\, \hat{u} \in \hat{E}\hat{H}^2_A(\Gamma) \oplus \widetilde{\widehat{H}}_A(\Gamma_h) \\ (u, A_h^* v)_h + c_h(\hat{u}, \hat{v}) = (f, v) - \langle f_D, \hat{v}\rangle_{\Gamma_h} \quad \forall v \in H_{A^*}(\Omega_h). \end{cases} \tag{2.41}$$

Note that, in both (2.40) and (2.41), $\hat{u}$ is independent unknown but $\hat{v}$ denotes the trace of broken test function $v \in H_{A^*}(\Omega_h)$.

The bilinear[15] form corresponding to the formulation,

$$b((u, \hat{u}), v) := (u, A_h^* v)_h + c_h(\hat{u}, v), \tag{2.42}$$

generates two corresponding operators:

$$b((u, \hat{u}), v) = \langle B(u, \hat{u}), v\rangle = \langle (u, \hat{u}), B'v\rangle. \tag{2.43}$$

The null space of conjugate operator B' coincides with the null space of $A^*|_V$. Indeed, let

$$b((u, \hat{u}), v) = 0 \quad \forall (u, \hat{u}). \tag{2.44}$$

Taking an arbitrary $\hat{u} \in \widetilde{\widehat{H}}_A(\Gamma_h)$, we conclude that v must be globally conforming, so the bilinear form in (2.44) reduces to that in (2.22).

The null space of DPG operator B consists of all $(u, \hat{u})$ such that

$$b((u, \hat{u}), v) = 0 \quad \forall v \in H_{A^*}(\Omega_h). \tag{2.45}$$

Similar to our approach with the ultra-weak variational formulation, here we first test with $v \in \mathcal{D}(\Omega)$ to conclude that $Au = 0$. Integrating the first term by parts and testing with arbitrary v, we conclude that $\hat{u} = u$ on Γ_h. In particular, as $\hat{u}|_\Gamma \in \hat{H}^2_A(\Gamma)$, this implies that $C_1\hat{u} = 0$ on Γ.

Our main abstract result follows.

Theorem 3. *Assume additionally that the range of A^* defined on the whole energy space $H_{A^*}(\Omega)$ coincides with $L^2(\Omega)$. Problem (2.41) is then well-posed. More precisely, for any data f, f_D satisfying the compatibility condition (2.23), the problem has a solution $(u, \hat{u})$ such that $(u, \hat{u}|_\Gamma)$ coincides with the solution of (2.21). The bilinear form satisfies the inf–sup condition*

$$\sup_{v \in H_{A^*}(\Omega_h)} \frac{|(u, A_h^* v)_h + c_h(\hat{u}, \hat{v})|}{\|v\|_{H_{A^*}(\Omega_h)}} \geq \gamma_{\mathrm{DPG}} \left(\|u\|^2_{L^2(\Omega)} + \|\hat{u}\|^2_{\hat{H}_A(\Gamma_h)} \right)^{1/2} \tag{2.46}$$

for all $\hat{u} \in \hat{E}\hat{H}^2_A(\Gamma) \oplus \widetilde{\widehat{H}}_A(\Gamma_h)$, and $u \in L^2(\Omega)$ orthogonal to the null space:

$$\{(u, \hat{u}) : u \in \mathcal{N}(A|_U) \text{ and } \hat{u} = u \text{ on } \Gamma_h\}. \tag{2.47}$$

The inf–sup constant γ_{DPG} is mesh-independent and of the same order as the inf–sup constant for the ultra-weak variational formulation. ■

Proof. We will switch the order of spaces in the inf–sup condition[16] and prove that

$$\sup_{u \in L^2(\Omega), \hat{u} \in \hat{E}\hat{H}^2_A(\Gamma) \oplus \widetilde{\widehat{H}}_A(\Gamma_h)} \frac{|(u, A_h^* v)_h + c_h(\hat{u}, \hat{v})|}{(\|u\|^2_{L^2(\Omega)} + \|\hat{u}\|^2_{\hat{H}_A(\Gamma_h)})^{1/2}} \geq \gamma_{\mathrm{DPG}} \|v\|_{H_{A^*}(\Omega_h)} \tag{2.48}$$

for all v L^2-orthogonal to $\mathcal{N}(A^*|_V)$.

14 That is, the ultra-weak variational formulation with broken test functions.

15 Sesquilinear for complex-valued problems.

16 In general, one may switch the order of the spaces in the inf–sup condition if the operator and its adjoint are both injective (see [32] for details). When the operator and its adjoint are not injective, we *make* them injective by considering quotient spaces instead (dividing through by the null space). In the Hilbert space setting, quotient spaces are isomorphic and isometric to orthogonal complements, our present setting.

Step 1: Consider first a special case when $A_h^* v = 0$. Consider a conforming $u \in (\mathcal{N}(A|_U))^\perp \subset U$ such that $Au = v$. As $v \in (\mathcal{N}(A^*|_V))^\perp$, such u exists. We then have

$$\begin{aligned}\|v\|^2 &= (Au, v) = \underbrace{(u, A_h^* v)}_{=0} + c_h(\operatorname{tr} u, v)\\ &\le \frac{|c_h(\operatorname{tr} u, \hat{v})|}{\|\operatorname{tr} u\|} \|\operatorname{tr} u\|\\ &\le \sup_{\hat{u}} \frac{|c_h(\hat{u}, \hat{v})|}{\|\hat{u}\|} \|u\|_{H_A(\Omega)}\\ &\le \frac{1}{\gamma} \sup_{\hat{u}} \frac{|c_h(\hat{u}, \hat{v})|}{\|\hat{u}\|} \|v\|. \end{aligned} \tag{2.49}$$

Dividing both sides by $\|v\|$, we get the required inequality.

Step 2: Now let v be arbitrary. Consider a conforming $\widetilde{v} \in H_{A^*}(\Omega)$ such that $A^*\widetilde{v} = A_h^* v$. By assumption, such a function always exists and can be interpreted as a solution to the strong adjoint problem with non-homogeneous BC data $f_D = C_2'\widetilde{v}$,

$$\begin{cases} A^*\widetilde{v} = A_h^* v \\ C_2'\widetilde{v} = f_D. \end{cases} \tag{2.50}$$

In order to ensure uniqueness and boundedness in the L^2-norm, we assume that $\widetilde{v}$ is L^2-orthogonal to the null space $\mathcal{N}(A^*|_V)$.

Now, by construction, $A_h(v - \widetilde{v}) = 0$ and $v - \widetilde{v} \in (\mathcal{N}(A^*|_V))^\perp$ so, by the Step 1 result, the difference $v - \widetilde{v}$ is bounded in both L^2 and H_{A^*} norms by the supremum in (2.48). We then have only to demonstrate that we can control the norm of the conforming $\widetilde{v}$. We can: if we restrict ourselves in (2.48) to conforming test functions, the bilinear form collapses to (2.22).

This finishes the proof. ■

2.4. DPG formulation for the Stokes problem

We begin by emphasizing the global character of the decomposition of traces in (2.34). The velocity trace $\hat{\boldsymbol{u}} \in \boldsymbol{H}^{1/2}(\Gamma_h)$ can be decomposed into an extension of $\hat{\boldsymbol{u}}_0$ on the boundary Γ and the trace on the internal skeleton Γ_h^0:

$$\hat{\boldsymbol{u}} = \hat{E}\hat{\boldsymbol{u}}_0 + \widetilde{\hat{\boldsymbol{u}}}.$$

In finite element computations, traces are approximated with functions that are globally continuous on the skeleton Γ_h. The trace $\hat{\boldsymbol{u}}_0$, which is known from the boundary condition, has to be lifted to the whole skeleton. In computations, we use finite element shape functions and lift $\hat{\boldsymbol{u}}_0$ only into the layer of elements neighboring Γ. The unknown part of velocity trace $\widetilde{\hat{\boldsymbol{u}}} \in \widetilde{\boldsymbol{H}}^{1/2}(\Gamma_h^0)$, by contrast, is defined only on the internal skeleton.

The unknown traction trace $\hat{\boldsymbol{t}} \in \boldsymbol{H}^{-1/2}(\Gamma_h)$ is defined on the entire skeleton. On the continuous level, the decomposition of traction into a lift of its restriction to Γ and the remaining component $\widetilde{\hat{\boldsymbol{t}}} \in \widetilde{\boldsymbol{H}}^{-1/2}(\Gamma)$ defined on the internal skeleton Γ_h^0 is also global. In 2D for instance, for $\boldsymbol{t}$ from a *standard* boundary space $\boldsymbol{H}^{-1/2}(\Gamma)$, the corresponding restriction to an edge e of an element K adjacent to boundary Γ lives only in $\boldsymbol{H}^{-1/2}(e)$ and *cannot* just be extended by zero to a functional in $\boldsymbol{H}^{-1/2}(\partial K)$. However, the conformity present in the definition of space $\boldsymbol{H}^{-1/2}(\Gamma_h)$ is so weak that it does not translate into any global continuity conditions for the approximating polynomial spaces that are discontinuous from edge to edge.

For the Stokes problem, the boundary operators represent exactly the velocity and traction components of the solution trace;

$$C_1(\hat{\boldsymbol{t}}, \hat{\boldsymbol{u}}) = \boldsymbol{u}, \qquad C_2(\hat{\boldsymbol{t}}, \hat{\boldsymbol{u}}) = \hat{\boldsymbol{t}}.$$

As discussed earlier, the difference between the two ways of imposing boundary conditions is in our case insignificant. The abstract $\langle f_D, v\rangle$ term corresponds to $\langle \boldsymbol{u}_D, \hat{\boldsymbol{r}}\rangle_\Gamma$, where $\hat{\boldsymbol{r}}$ is the traction component of the test function. Its extension to discontinuous test functions v is constructed by lifting Dirichlet data $\boldsymbol{u}_D$ to the whole skeleton. The first way of imposing boundary conditions is essentially the same: the abstract lift $\hat{u}_0$ of $\boldsymbol{u}_D$ can be selected to be $(\boldsymbol{u}_D, \boldsymbol{0})$ (zero traction) and, if we use the same extension of $\boldsymbol{u}_D$ to the whole skeleton, the two formulations will be identical. As in classical finite element computations, we may or may not interpolate data $\boldsymbol{u}_D$ in the finite element space. Suppose, for example, that we approximate traces with quadratics and have non-polynomial data $\boldsymbol{u}_D$. We could first interpolate the data with quadratics and use quadratic shape functions to lift the data to the whole skeleton. The contributions to the load vector would be computed by integrating the quadratic lifts against test functions. Alternately, we might integrate the non-polynomial $\boldsymbol{u}_D$ on Γ directly against the test functions—in general, this will yield different values. Additionally, even if we lift the non-polynomial $\boldsymbol{u}_D$ to the whole skeleton with the same quadratic shape functions, the lifts would differ on the internal skeleton and, consequently, the resulting approximate traces would differ. In the limit, of course, the difference would disappear.

The null space of conjugate operator B' coincides with the null space of adjoint A^* with homogeneous boundary conditions $\boldsymbol{v} = \boldsymbol{0}$ on Γ and consists of constant pressures

$$\{(\boldsymbol{0}, c, \boldsymbol{0}) : c \in \mathbb{R}\}.$$

The null space of operator B is the same as that for the operator corresponding to the ultra-weak formulation,

$$\{((\boldsymbol{u}, p, \boldsymbol{\sigma}), \hat{\boldsymbol{t}}) : \boldsymbol{u} = \boldsymbol{0}, p = c, \boldsymbol{\sigma} = \boldsymbol{0}, \hat{\boldsymbol{t}} = c\boldsymbol{n} \text{ where } c \in \mathbb{R}\}.$$

The non-trivial null spaces imply the compatibility condition for the load and non-uniqueness of the solution. The compatibility condition for the load involves the right-hand side g of the divergence equation[17] and the velocity trace boundary data $\boldsymbol{u}_D$, and takes the form

$$\int_\Omega g = \int_\Gamma \boldsymbol{u}_D \cdot \boldsymbol{n}.$$

This well-known condition can be obtained immediately by integrating the divergence equation and using the boundary condition on $\boldsymbol{u}$:

$$\int_\Omega g = \int_\Omega \operatorname{div} \boldsymbol{u} = \int_\Gamma \boldsymbol{u} \cdot \boldsymbol{n} = \int_\Gamma \boldsymbol{u}_D \cdot \boldsymbol{n}.$$

The assumption on surjectivity of the adjoint operator in Theorem 3 thus reduces to the condition that the divergence operator is surjective, a well-known fact.

With data satisfying the compatibility condition, the solution (pressure and tractions) is determined up to a constant. In computations, the constant can be fixed by implementing an additional scaling condition. We can enforce, for instance, zero average pressure in one particular element, or zero average normal traction on a particular edge. The scaling will affect the ultimate values for pressure and tractions, but has no effect on the velocity or on its gradient and trace.

2.5. A summary

We have studied the well-posedness of the ultra-weak variational formulation with broken test spaces (the DPG formulation) for a first-order system of PDEs equivalent to the classical Stokes problem. We have employed an abstract notation corresponding to the classical theory of L^2-adjoint operators. In addition to the presented Stokes example, the theory covers a number of boundary-value problems studied earlier, including Poisson, convection–diffusion, elasticity, and linear acoustics problems [9,22,23]. The present effort at the abstract level focuses on (a) non-homogeneous boundary data, (b) the possible non-uniqueness of the solution, and (c) relation with the classical theory of L^2-adjoints for closed operators.

While we make no claims as to the generality of the presented abstract framework, we believe that the presented theory may guide the study of arbitrary systems of first-order systems of PDEs. In the course of our reasoning, we have made a number of abstract assumptions that have been verified for the Stokes problem, which we now summarize.

- Operator A^* defined on the graph energy space is surjective (required for Theorem 3).
- Both energy graph spaces $H_A(\Omega)$ and $H_{A^*}(\Omega)$ admit corresponding trace spaces $\hat{H}_A(\partial\Omega)$, $\hat{H}_{A^*}(\partial\Omega)$.
- The boundary bilinear (sesquilinear) term $c(u, v)$ resulting from integration by parts is definite.
- Boundary operator C_1 is defined in such a way that Assumption (2.14) is satisfied.
- With homogeneous boundary condition $C_1 u = 0$ in place, operator A is bounded below in the L^2-orthogonal complement of its null space.

With these conditions satisfied, the DPG formulation is well-posed. The corresponding inf–sup constant is mesh-independent. Neglecting technical details, the central message is this: *the boundedness below of the strong operator with homogeneous boundary conditions implies the inf–sup condition for the DPG formulation with a mesh-independent constant*.

The general theory guides our definition of unknown traces on the skeleton. The energy setting involves graph norms for both operator A and its formal adjoint A^*. The graph norm on the test space is equivalent to the *optimal test norm* [5] with *mesh-independent* equivalence constants. The graph norm for A determines the energy setting for unknown traces and the minimum-energy extension norm.

3. Numerical experiments

To illustrate the theoretical results, we perform three numerical experiments. In the first two we use boundary conditions and forcing function corresponding to a manufactured solution; first showing optimal convergence using the graph norm

[17] $g = 0$ in practice.

arising from the analysis as the test space norm, then showing sub-optimal convergence when a naive norm is selected instead. Finally, we examine the classic lid-driven cavity flow problem.

We implemented the experiments described below using *Camellia*, a toolbox for DPG developed by Roberts starting at Sandia in summer 2011, in collaboration with Denis Ridzal and Pavel Bochev [16]. Camellia supports 2D meshes of triangles and quads of variable polynomial order, provides mechanisms for easy specification of DPG variational forms, supports *h*- and *p*-refinements, and supports distributed computation of the stiffness matrix, among other features.

Recall that the pressure p in the Stokes problem is only determined up to a constant. Following a method described by Bochev and Lehoucq [33], we add a constraint on the pressure that enforces

$$\int_\Omega p = 0,$$

thereby determining the solution uniquely. This constraint is also satisfied by the manufactured solution used in our experiments.

Before turning to the experiments themselves, we briefly note the expected convergence properties and give a few implementation details. When implementing DPG, we have several choices: what polynomial orders to use for the approximation of fields, traces, and fluxes; how to approximate the optimal test functions, and what norm to use on the test space. We discuss each of these in turn.

3.1. Convergence and orders of polynomial approximation

For a DPG solution $(u_h, \widehat{u}_h)$ and exact solution $(u, \widehat{u})$, the analysis in Section 2 gives us

$$\left(\|u - u_h\|^2 + \|\widehat{u} - \widehat{u}_h\|^2_{\hat{H}_A(\Gamma_h)}\right)^{1/2} \leq \frac{M}{\gamma_{\text{DPG}}} \inf_{(w_h, \widehat{w}_h)} \left(\|u - w_h\|^2 + \|\widehat{u} - \widehat{w}_h\|^2_{\hat{H}_A(\Gamma_h)}\right)^{1/2}. \tag{3.51}$$

In fact, according to the analysis from the previous section, for the DPG formulation (ultraweak variational formulation with broken test spaces), the continuity constant $M = 1$, and the inf–sup constant γ_{DPG} is of order of Friedrichs constant[18] γ and inf–sup constant δ for the BC operator C_1. The result holds only for *exact* optimal test functions; we neglect the error due to their approximation with enriched spaces. The salient point for convergence is that these are mesh-independent constants: for the graph norm presented in the analysis, the method is automatically stable.[19]

Assuming u is sufficiently smooth, for a discrete L^2 space comprised of polynomials of order k, we expect best *h*-convergence rates of $k + 1$; that is, we have

$$\inf_{w_h \in U_h} \|u - w_h\| \leq C_1 h^{k+1} \tag{3.52}$$

for some mesh-independent constant C_1. It can be shown that, for traces $\widehat{w}_h$ whose $H^{-1/2}(\Gamma_h)$ and $H^{1/2}(\Gamma_h)$ components are approximated by polynomials of orders k and $k + 1$, respectively,

$$\inf_{\widehat{w}_h \in \hat{H}_A(\Gamma_h)} \|\widehat{u} - \widehat{w}_h\|_{\hat{H}_A(\Gamma_h)} \leq C_2 h^{k+1}$$

for some mesh-independent constant C_2. For details and further references, see [9, pp. 7–8]. Combining this with Eqs. (3.51) and (3.52), we then have the bound

$$\|u - u_h\| \leq C h^{k+1}$$

for $C = \min(C_1, C_2)$. Assuming negligible error in computing the optimal test functions, for these choices of polynomial order, we expect DPG solutions to converge in h at the optimal rate of $k + 1$ for all L^2 variables.

We can also motivate the choice of polynomial orders for the trial space intuitively from the exact sequence. If we define k as the polynomial order of approximation of field variables, because these belong to L^2, it is natural to choose $k + 1$ as the H^1 order. The traces of H^1 functions ($\widehat{u}_1$ and $\widehat{u}_2$) belong to $H^{1/2}$, a stronger space than L^2, so that $k + 1$ is a natural order of approximation for these. The traces of $H(\text{div})$ functions $\left(\widehat{\begin{pmatrix}\sigma_{11}-p\\ \sigma_{12}\end{pmatrix}} \cdot \boldsymbol{n} \text{ and } \left(\widehat{\begin{pmatrix}\sigma_{21}\\ \sigma_{22}-p\end{pmatrix}} \cdot \boldsymbol{n}\right)\right.$ belong to $H^{-1/2}$, a weaker space than L^2, so that k is a natural order of approximation for these.

The exact optimal test functions will not in general be polynomials; we approximate them by using an "enriched" space of Lagrange and Raviart–Thomas elements approximating $H^1(\Omega_h)$ and $\boldsymbol{H}(\text{div}, \Omega_h)$ components of the test space. In practice, we experiment with various levels of enrichment, and take the minimum enrichment that yields results nearly as good as higher levels of enrichment. In the present work, we used 1 as the enrichment order; that is, $k_{\text{test}} = k + 2$. As will be seen

18 I.e., the inf–sup constant for operator $A|_U$.

19 As will be seen in what follows, if we use the naive test norm instead, we do *not* get the optimal convergence rates in the pressure. We hypothesize that if we performed a similar analysis for the naive norm, γ would not be mesh-independent.

below, with this, we come extremely close to matching the best approximation error, so that there is no benefit to enriching the test space further.[20]

Note also that we have made no assumptions about the choice of basis functions. The present work uses H^1- and $H(\mathrm{div})$-conforming nodal bases provided by the Intrepid package in Trilinos [34].

3.2. Test space norm

The choice of test norm arising from the above analysis is the (adjoint) graph norm:

$$\|(\boldsymbol{\tau}, \boldsymbol{v}, q)\|^2_{\text{graph}} = \|\nabla \cdot \boldsymbol{\tau} - \nabla q\|^2 + \|\nabla \cdot \boldsymbol{v}\|^2 + \|\boldsymbol{\tau} + \nabla \boldsymbol{v}\|^2 + \|\boldsymbol{\tau}\|^2 + \|\boldsymbol{v}\|^2 + \|q\|^2 .$$

We use this norm in our first experiment, and get the optimal convergence rates for the field variables. In our second experiment, we consider another choice of test norm, which we refer to as the *naive* test space norm:

$$\|(\boldsymbol{\tau}, \boldsymbol{v}, q)\|^2_{\text{naive}} = \|\boldsymbol{\tau}\|^2 + \|\nabla \cdot \boldsymbol{\tau}\|^2 + \|\boldsymbol{v}\|^2 + \|\nabla \boldsymbol{v}\|^2 + \|q\|^2 + \|\nabla q\|^2 .$$

Note that this is a *stronger* space than the one generated by the graph norm; that is, if we define

$$V_{\text{graph}} = \{(\boldsymbol{\tau}, \boldsymbol{v}, q) : \|(\boldsymbol{\tau}, \boldsymbol{v}, q)\|_{\text{graph}} < \infty\}, \quad \text{and}$$
$$V_{\text{naive}} = \{(\boldsymbol{\tau}, \boldsymbol{v}, q) : \|(\boldsymbol{\tau}, \boldsymbol{v}, q)\|_{\text{naive}} < \infty\},$$

then $V_{\text{naive}} \subset V_{\text{graph}}$. Specifically, V_{graph} only requires $\nabla \cdot \boldsymbol{\tau} - \nabla q \in \boldsymbol{L}^2$, while V_{naive} requires $\nabla \cdot \boldsymbol{\tau} \in \boldsymbol{L}^2$ *and* $\nabla q \in \boldsymbol{L}^2$.

3.3. Manufactured solution experiment with graph test space norm

To test the method, we use a manufactured solution following Cockburn et al. [35]

$$u_1 = -e^x(y \cos y + \sin y)$$
$$u_2 = e^x y \sin y$$
$$p = 2\mu e^x \sin y$$

on domain $\Omega = (-1, 1)^2$, taking $\mu = 1$, with uniform quadrilateral meshes of increasing granularity, and examine convergence rates. The L^2 norm of the exact solution for u_1 is 2.53; for u_2, 1.07; for p, 2.81.

Figs. 1 and 2 show h- and p-convergence[21] results using the graph norm in the test space, for uniform quadrilateral meshes varying from $k = 1$ to 4 in polynomial order, and from 1×1 to 16×16 elements. The dashed lines in the plots show the error of an L^2 projection of the exact solution (the theoretical best we could achieve)—the lines lie nearly on top of each other. We not only observe optimal convergence rates, but almost exactly achieve the best approximation error!

3.4. Manufactured solution experiment with naive test space norm

Our second manufactured solution experiment uses the naive norm on the test space. This was the first norm we used when studying DPG formulations of Stokes [8], before we had developed the analysis above, showing why the naive norm might not do as well as the graph norm does.

Figs. 3 and 4 show h- and p-convergence results using the naive norm in the test space, for uniform quadrilateral meshes varying from $k = 1$ to 4 in polynomial order, and from 1×1 to 16×16 elements; we have again plotted for comparison the error in the L^2 projection of the exact solution. As with the graph norm, here we observe optimal convergence rates and almost exactly achieve the best approximation error in velocities u_1 and u_2, but in the pressure p we are sub-optimal by up to two orders of magnitude.

Why do we not see optimal convergence for the naive norm? Recall that this is a stronger norm than the graph norm used in our analysis; thus the test functions that we seek – namely, the ones that will minimize the residual – may not reside within the continuous space represented by the naive norm. By using the naive norm, we are searching for these test functions inside a smaller space, and we may not find them there.

3.5. Lid-driven cavity flow

A classic test case for Stokes flow is the lid-driven cavity flow problem. Consider a square cavity with an incompressible, viscous fluid, with a lid that moves at a constant rate. The resulting flow will be vorticular; as sketched in Fig. 5, there will also be so-called *Moffatt eddies* at the corners; in fact, the exact solution will have an infinite number of such eddies, visible

[20] For an analysis of the effect of the test space enrichment on rates of convergence in the Laplace problem and linear elasticity, see Gopalakrishnan and Qiu [13].

[21] In this context, by p we mean polynomial refinements. We mostly use k for polynomial order, because p is our pressure variable; but a few times in the following pages we will overload p to mean polynomial order as well.

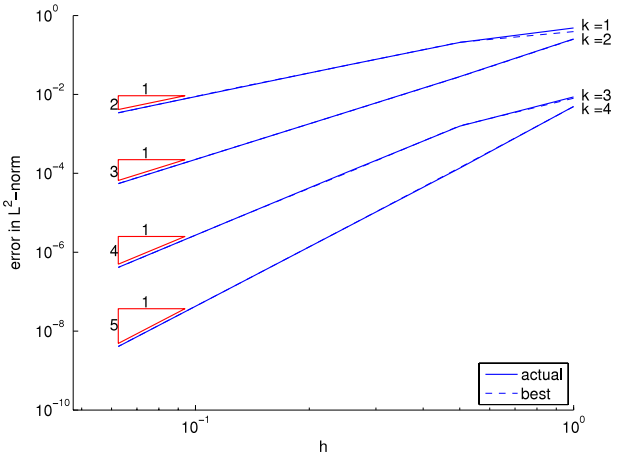

(a) u_1.

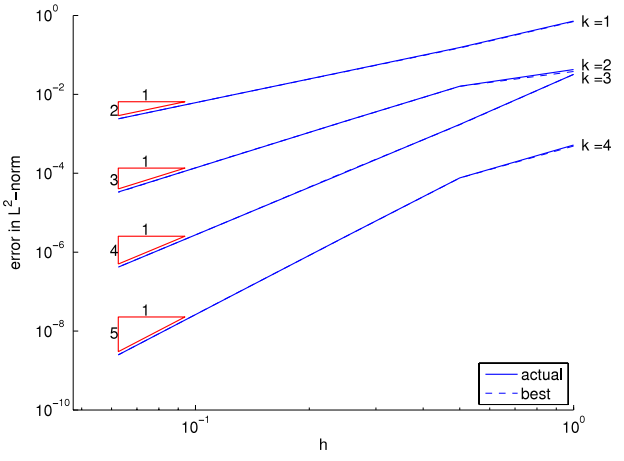

(b) u_2.

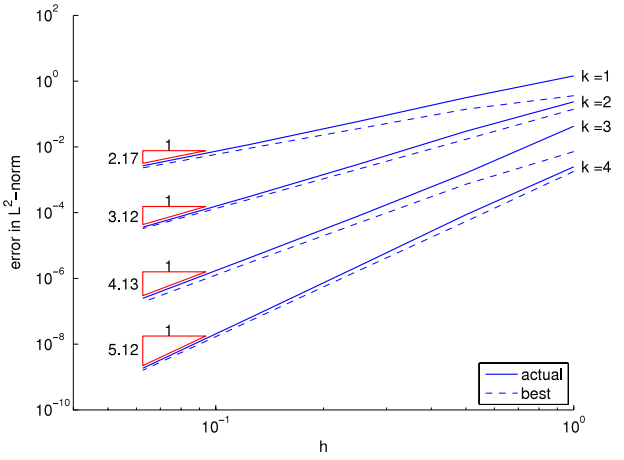

(c) p.

Fig. 1. h-convergence of u_1, u_2 and p when using the graph norm for the test space. We observe optimal convergence rates, and nearly match the L^2-projection of the exact solution.

at progressively finer scales [36]. Note that the problem as described will have a discontinuity in the fluid velocity at the top corners, and hence its solution will not conform to the spaces we used in our analysis; for this reason, in our experiment we

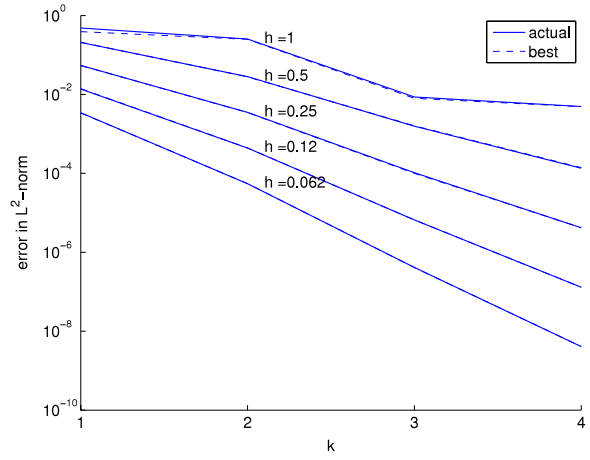

(a) u_1.

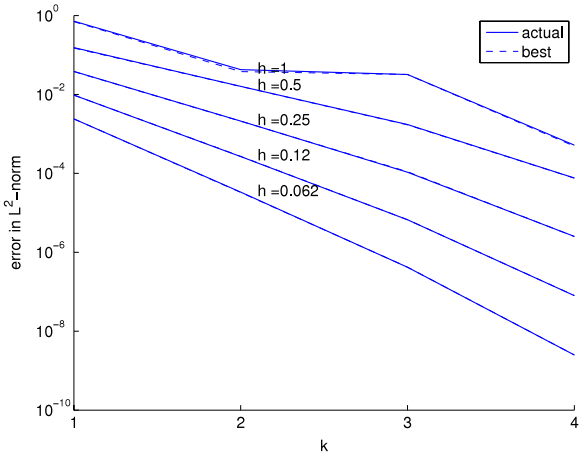

(b) u_2.

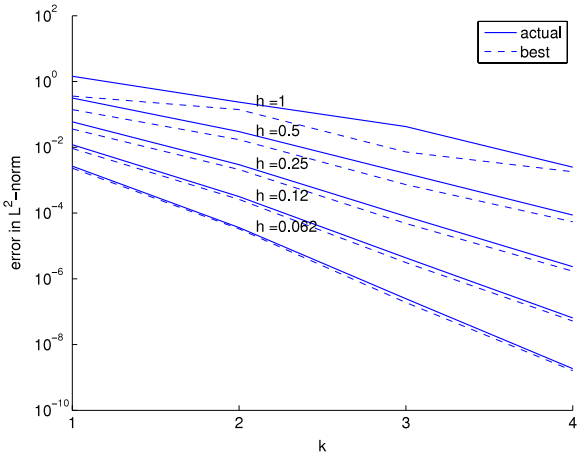

(c) p.

Fig. 2. p-convergence of u_1, u_2 and p when using the graph norm for the test space. We observe exponential convergence for the finer meshes, and nearly match the L^2-projection of the exact solution.

approximate the problem by introducing a thin ramp in the boundary conditions—we have chosen a ramp of width $\frac{1}{64}$. This makes the boundary conditions continuous,[22] so that the solution conforms to the spaces used in the analysis.

As described in the introduction, DPG gives us a mechanism for measuring the residual error in the dual norm (the very error we seek to minimize) precisely, and we use this to drive adaptivity, by measuring the error $\|e_K\|_V$ for each element K. Both the method and our code allow refinements in h or p or in some combination of h and p. However, we do not yet have a general mechanism for deciding *which* refinement to apply (h or p), once we have decided that a given element should be refined. We run two experiments, one with h-adaptivity and one using an ad hoc hp-adaptive strategy, described below.

Although it is not required by the code, we enforce 1-*irregularity* throughout—that is, before an element can be refined twice along an edge, its neighbor along that edge must be refined once. In limited comparisons running the same experiments without enforcing 1-irregularity, this did not appear to make much practical difference.

3.5.1. h-refinement strategy

For h-refinements, our strategy is very simple:

1. Loop through the elements, determining the maximum element error $\|e_{K\max}\|_V$.
2. Refine all elements with error at least 20% of the maximum $\|e_{K\max}\|_V$.

22 It is worth noting that these boundary conditions are not exactly representable by many of the coarser meshes used in our experiments. We interpolate the boundary conditions in the discrete space.

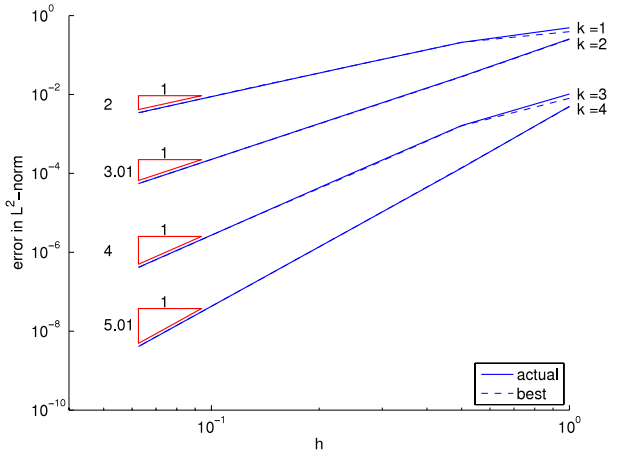

(a) u_1.

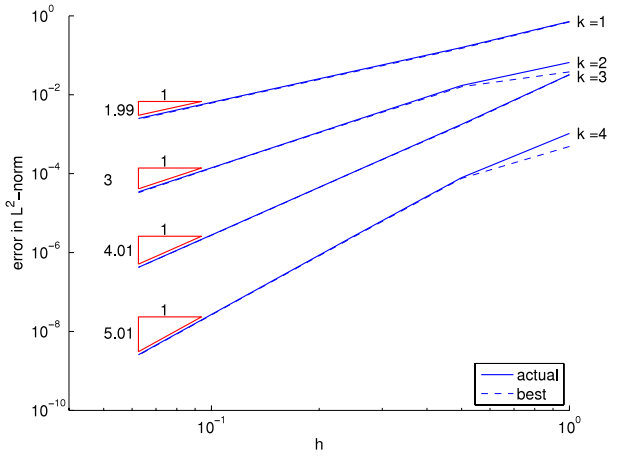

(b) u_2.

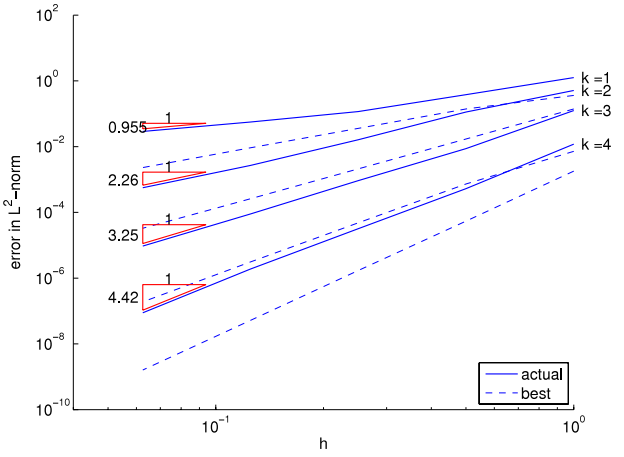

(c) p.

Fig. 3. h-convergence of u_1, u_2 and p when using the naive norm for the test space. We observe optimal convergence rates (and nearly match the L^2-projection of the exact solution) for u_1 and u_2, but p converges at suboptimal rates.

Because the exact solution is unknown, we first solve on an overkill mesh and compare our adaptive solution at each step to the overkill solution. In this experiment, we used quadratic field variables ($k = 2$), a test space enrichment of 1 relative

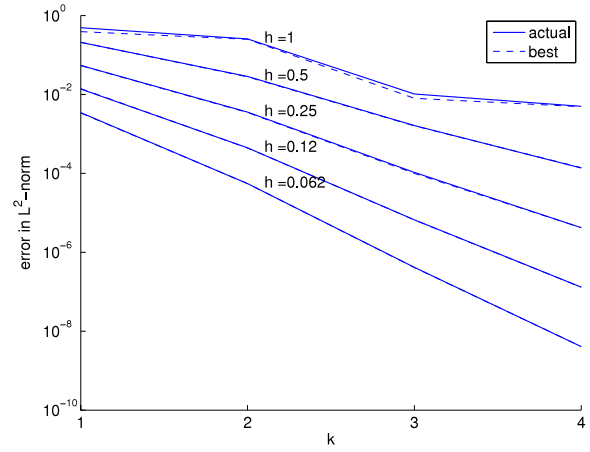

(a) u_1.

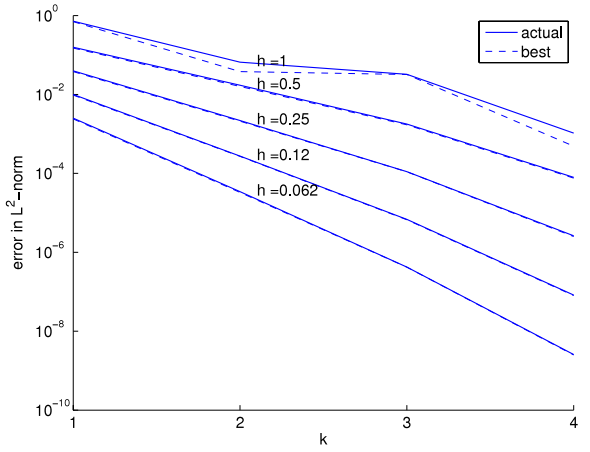

(b) u_2.

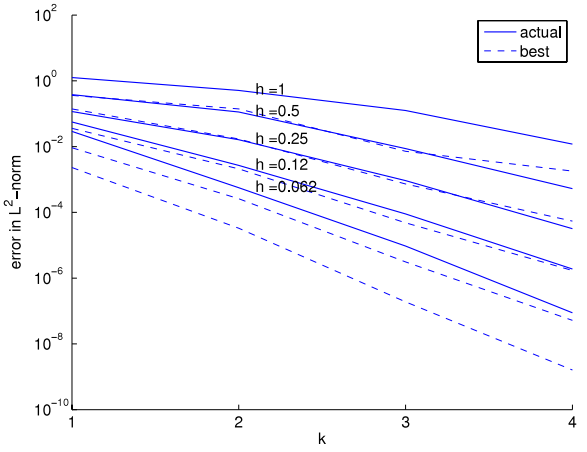

(c) p.

Fig. 4. p-convergence of u_1, u_2 and p when using the naive norm for the test space. We observe exponential convergence for the finer meshes, and nearly match the L^2-projection of the exact solution for u_1 and u_2, but see significantly suboptimal solutions in p.

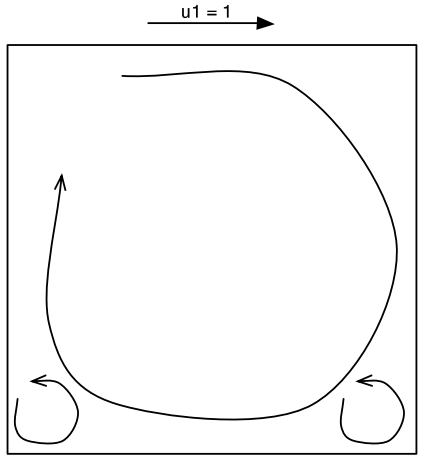

Fig. 5. Sketch of lid-driven cavity flow.

to the H^1 order (that is, $k_{\text{test}} = k + 2 = 4$) for both the adaptive and overkill solutions. The overkill mesh was 256×256 elements, with 5,576,706 dofs.

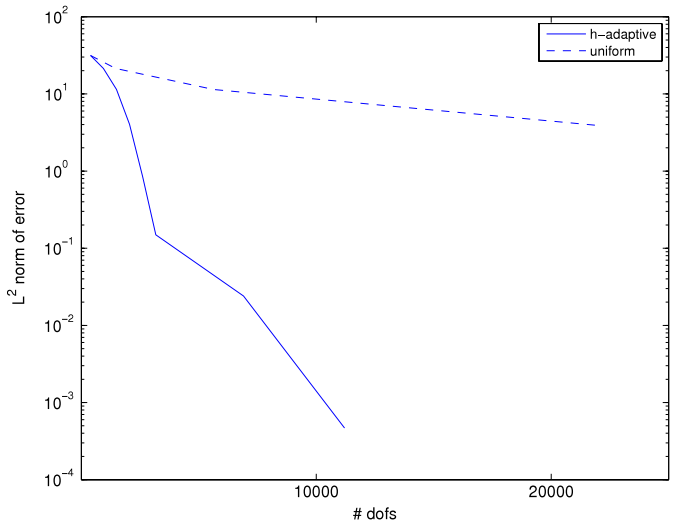

Fig. 6. Euclidean norm of L^2 error in all field variables in h-adaptive mesh relative to an overkill mesh with 256×256 quadratic elements. The Euclidean norm of all field variables in the exact solution is 6.73.

The initial mesh was a 2×2 square mesh; we ran seven h-adaptive refinements. We stopped after seven steps to ensure that the resulting mesh was nowhere finer than the overkill solution. At each step, we computed the Euclidean (ℓ_2) norm of the L^2 norm of each of the seven field variables. The final adaptive mesh has 124 elements and 11,202 dofs, and combined L^2 error of 4.4×10^{-4} compared with the overkill mesh. We also ran a few uniform refinements and computed the L^2 error for these compared with the overkill mesh, to show the comparative efficiency of the adaptive refinements. The results are plotted in Fig. 6.

We also post-processed the results to solve for the stream function ϕ, where $\Delta\phi = \nabla \times \boldsymbol{u}$. The contours of ϕ are the streamlines of the flow. These are plotted for the quadratic adaptive mesh described above in Fig. 7; the first Moffatt eddy can be seen clearly in the zoomed-in plot. This quadratic mesh does not resolve the second Moffatt eddy, but if we run 11 adaptive refinements on a cubic mesh, we can see it. This is shown in Fig. 8.

3.5.2. Ad hoc hp-refinement strategy

For the *hp* experiment, we adopt a similar strategy; this time, our overkill mesh contains 64×64 quintic elements, and our initial mesh has 2×2 linear elements. We know *a priori* that we should refine in h at the top corners—if only to fully resolve the boundary condition. The strategy is again:

1. Loop through the elements, determining the maximum element error $\|e_{K\max}\|_V$.
2. Refine all elements with error at least 20% of the maximum $\|e_{K\max}\|_V$.

However, this time we must decide whether to refine in h or p. The basic constraints we would like to follow are:

- the adaptive mesh must be nowhere finer than the overkill mesh (in h or p), and
- prefer h-refinements at all corners (top and bottom).

So, once the corner elements are as small as the overkill mesh, then they refine in p, and all other elements refine in p until they are quintic, after which they may refine in h.

The primary purpose of this experiment is to demonstrate that the method allows arbitrary meshes of arbitrary, variable polynomial order. The strategy described above clearly depends on *a priori* knowledge of the particular problem we are solving; we have yet to determine a good general strategy for deciding between h- and p-refinements.

We ran 9 refinement steps. The final mesh has 46 elements and 5986 dofs, compared with 1,223,682 dofs in the overkill mesh. The L^2 error of the adaptive solution compared with the overkill is 8.0×10^{-4}. As in the previous experiment, we also tried running a few uniform h-refinements on the same initial mesh, as a baseline for comparison. The results are plotted in Fig. 9; the mesh can be seen in Fig. 10.

4. Conclusion

In this paper, we have presented a general framework for the analysis of DPG problems, and have applied that framework to a formulation of the Stokes problem to show its well-posedness. Without any Stokes-specific tricks, the method achieves

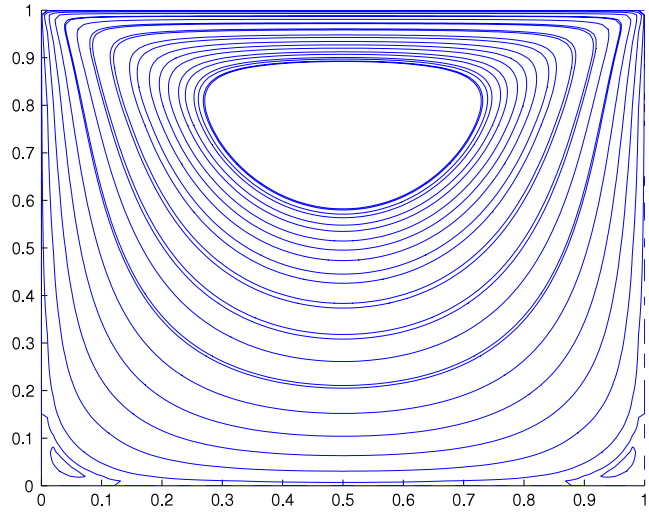

(a) Full cavity.

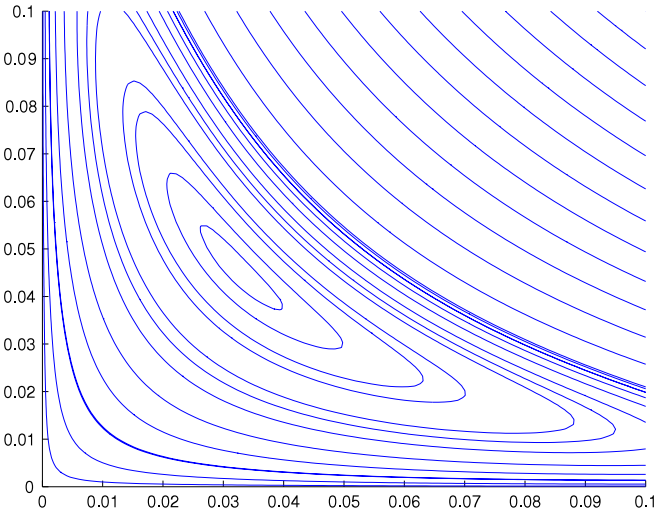

(b) Lower-left corner.

Fig. 7. Streamlines for the full cavity and for the lower-left corner, on a quadratic mesh after 7 adaptive refinements. The lower-left corner shows the first Moffatt eddy. The final mesh has 124 elements and 11,202 dofs.

optimal convergence with equal orders in velocity and pressure—it even comes very close to the best approximation in the discrete space. We have demonstrated with numerical experiments the power of adaptivity in both h and p.

In future works, we would like to extend the analysis to other first-order Stokes formulations. The velocity–vorticity–pressure (VVP) formulation from [16] has the particular advantage of parsimony in the number of variables; whereas the present formulation requires 7 field variables, the VVP formulation requires only 4 field variables; both formulations involve 2 traces and 2 fluxes.

We would also like to account more precisely in our analysis for the approximation of optimal test functions. We achieved near-optimal results here with a minimal test space enrichment; can we prove that this will suffice for all admissible forcing functions and boundary conditions? A similar question arises with respect to the asymptotic convergence: it appears from our numerical experiments that the solutions converge to the best approximations, with a scaling constant of 1. If this is true, we would like to prove it.

We would like to extend the present work to related problems. In particular, we plan to investigate the Oseen equations and the incompressible Navier–Stokes equations in the near future. For the Oseen equations, which involve a linear approximation to the nonlinear convection term in Navier–Stokes, we expect that a nearly identical approach to the one that we have taken for Stokes will work well. For the Navier–Stokes equations, we hope to apply the minimum-residual approach directly to the nonlinear problem, perhaps in a similar fashion to the work by Moro et al. [15].

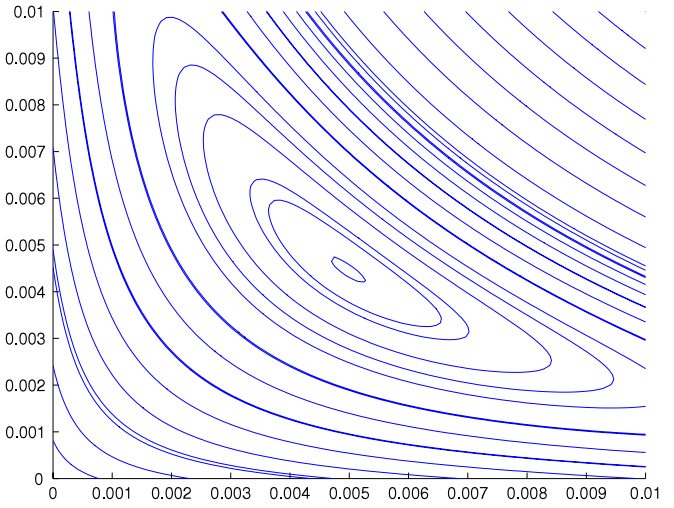

Fig. 8. Streamlines for the lower-left corner on a cubic mesh after 11 adaptive refinements: the second Moffatt eddy. The final mesh has 298 elements and 44,206 dofs.

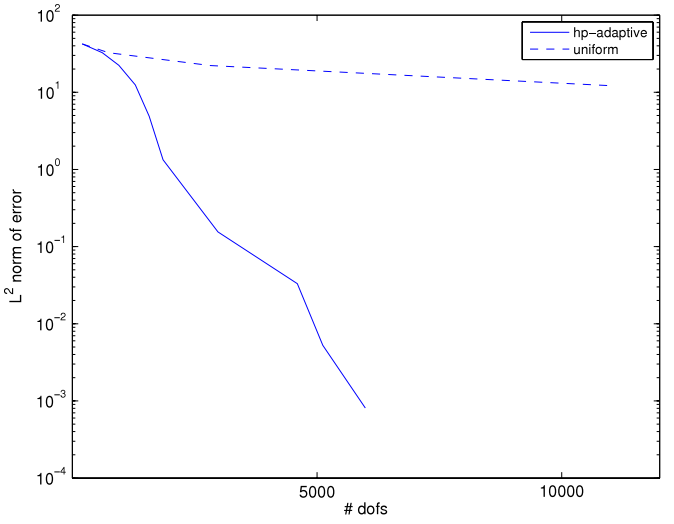

Fig. 9. Euclidean norm of L^2 error in all field variables in (ad hoc) *hp*-adaptive mesh relative to an overkill mesh with 64×64 quintic elements. The Euclidean norm of all field variables in the exact solution is 6.73; the final mesh has 46 elements and 5986 dofs.

Acknowledgments

Roberts and Demkowicz were supported by the Department of Energy (National Nuclear Security Administration) under Award Number (DE-FC52-08NA28615). We also thank Pavel Bochev and Denis Ridzal for hosting and collaborating with Roberts in the summers of 2010 and 2011, when he was supported by internships at Sandia National Laboratories (Albuquerque). We acknowledge with sincere thanks the second anonymous reviewer, whose wonderful work helped to improve the overall quality of the paper.

Appendix. Boundedness below of the first-order Stokes operator with homogeneous BCs

In this appendix, we show that the operator corresponding to our first-order Stokes problem with homogeneous BCs is bounded below. While in the body of the paper we have taken $\mu = 1$, here we consider the more general case of constant $\mu > 0$.

Recall the classical strong form of the Stokes problem:

$$-\mu\Delta\boldsymbol{u} + \nabla p = \boldsymbol{f} \quad \text{in } \Omega, \tag{A.53}$$

$$\nabla \cdot \boldsymbol{u} = 0 \quad \text{in } \Omega, \tag{A.54}$$

$$\boldsymbol{u} = \boldsymbol{u}_D \quad \text{on } \partial\Omega. \tag{A.55}$$

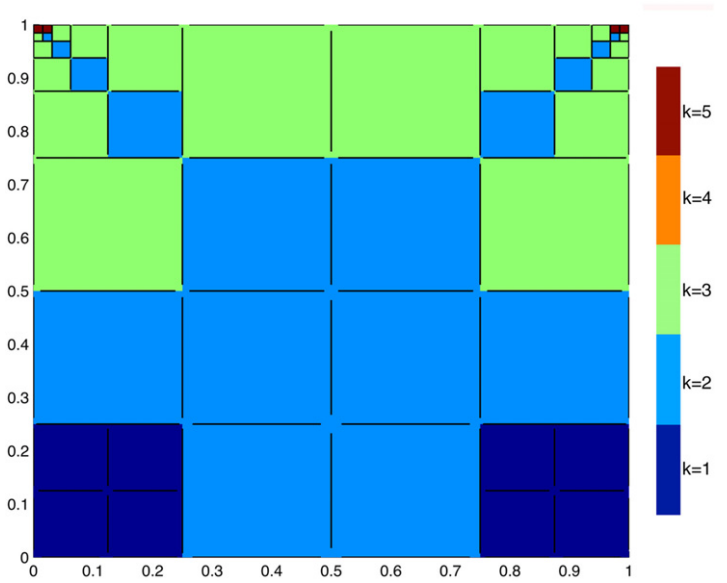

Fig. 10. Adaptive mesh for ad hoc *hp*-adaptivity strategy after 9 refinement steps. The scale represents the polynomial order of the L^2 variables in the solution. The final mesh has 46 elements and 5986 dofs.

Recall also our first-order system for the Stokes equations:

$$-\nabla \cdot \boldsymbol{\sigma} + \nabla p = \boldsymbol{f} \quad \text{in } \Omega, \tag{A.56a}$$

$$\nabla \cdot \boldsymbol{u} = \boldsymbol{0} \quad \text{in } \Omega, \tag{A.56b}$$

$$\frac{1}{\mu}\boldsymbol{\sigma} - \nabla \boldsymbol{u} = 0 \quad \text{in } \Omega, \tag{A.56c}$$

$$\boldsymbol{u} = \boldsymbol{u}_D \quad \text{on } \partial\Omega. \tag{A.56d}$$

If we introduce $A : H_A \to \boldsymbol{L}^2$ with group variable $u = (\boldsymbol{u}, p, \boldsymbol{\sigma})$, the Stokes equation in first order form (A.56), ignoring the boundary conditions, can be written succinctly as

$$Au \overset{\text{def}}{=} \begin{bmatrix} -\nabla \cdot \boldsymbol{\sigma} + \nabla p \\ \nabla \cdot \boldsymbol{u} \\ \frac{1}{\mu}\boldsymbol{\sigma} - \nabla \boldsymbol{u} \end{bmatrix} = \begin{bmatrix} \boldsymbol{f} \\ 0 \\ \boldsymbol{0} \end{bmatrix}. \tag{A.57}$$

Considering linear operator A as defined in Eq. (A.57) operating on group variable $u = (\boldsymbol{u}, p, \boldsymbol{\sigma})$, we seek to show that $\|Au\|_{L^2} \geq \gamma \|u\|_{H_A}$. Adding right-hand sides g and $\boldsymbol{h}$

$$-\nabla \cdot \boldsymbol{\sigma} + \nabla p = \boldsymbol{f} \quad \text{in } \Omega, \tag{A.58}$$

$$\nabla \cdot \boldsymbol{u} = g \quad \text{in } \Omega, \tag{A.59}$$

$$\frac{1}{\mu}\boldsymbol{\sigma} - \nabla \boldsymbol{u} = \boldsymbol{h} \quad \text{in } \Omega, \tag{A.60}$$

$$\boldsymbol{u} = \boldsymbol{0} \quad \text{on } \partial\Omega, \tag{A.61}$$

we have that $Au = (\boldsymbol{f}, g, \boldsymbol{h})$. If we can establish bounds for the L^2 norms of each of the solution variables in terms of L^2 norms on $\boldsymbol{f}$, g, and $\boldsymbol{h}$, then we will have the required lower bound $\|Au\|_\Omega \geq \gamma \|u\|_{H_A}$, where $\|u\|_{H_A} \overset{\text{def}}{=} \left(\|Au\|_\Omega^2 + \|u\|_\Omega^2\right)^{1/2}$.

Note that, by linearity of A, it suffices to consider cases in which only one of $\boldsymbol{f}$, g, and $\boldsymbol{h}$ is non-zero. We consider each of these cases in turn.

$\boldsymbol{f} \neq \boldsymbol{0}, g = 0, \boldsymbol{h} = \boldsymbol{0}$. In this case, we have exactly the system (A.56a)–(A.56d), which reduces (in a distributional sense) to (A.53)–(A.55). Testing the first equation with the velocity $\boldsymbol{u} \in \boldsymbol{H}_0^1(\Omega)$, we have

$$-(\mu \Delta \boldsymbol{u}, \boldsymbol{u})_\Omega + (\nabla p, \boldsymbol{u})_\Omega = (\boldsymbol{f}, \boldsymbol{u})_\Omega.$$

Integrating by parts, we obtain:

$$(\mu \nabla \boldsymbol{u}, \nabla \boldsymbol{u})_\Omega - \langle \mu \nabla \boldsymbol{u} \cdot \boldsymbol{n}, \boldsymbol{u} \rangle_{\partial\Omega} - (p, \nabla \cdot u)_\Omega + \langle p, \boldsymbol{u} \cdot \boldsymbol{n} \rangle_{\partial\Omega} = (\boldsymbol{f}, \boldsymbol{u})_\Omega.$$

Noting that $\boldsymbol{u} = 0$ on $\partial\Omega$ and that $\nabla \cdot \boldsymbol{u} = 0$ in Ω, this reduces to:

$$\begin{aligned}\mu(\nabla \boldsymbol{u}, \nabla \boldsymbol{u})_\Omega &= \mu \|\nabla \boldsymbol{u}\|_\Omega^2 = \mu \|\boldsymbol{\sigma}\|_\Omega^2 = (\boldsymbol{f}, \boldsymbol{u})_\Omega \\ &\leq \|f\|_\Omega \|\boldsymbol{u}\|_\Omega \\ &\leq C_P \|f\|_\Omega \|\nabla \boldsymbol{u}\|_\Omega,\end{aligned}$$

where C_P is the Poincaré constant. Thus $\|\boldsymbol{\sigma}\|_\Omega \leq \frac{C_P}{\mu}\|f\|_\Omega$, and $\|\boldsymbol{u}\| \leq \frac{C_P^2}{\mu}\|f\|_\Omega$.

To bound the pressure p, we require the inf–sup condition (which holds for Lipschitz as well as more general domains, as discussed in Section 2.2 of [37]) for $p \in L_0^2 \overset{\text{def}}{=} \{w \in L^2(\Omega) : \int_\Omega w = 0\}$:

$$\sup_{\boldsymbol{v} \in \boldsymbol{H}^1(\Omega)} \frac{(p, \nabla \cdot \boldsymbol{v})_\Omega}{\|\boldsymbol{v}\|_{H^1(\Omega)}} \geq \beta \|p\|_\Omega \tag{A.62}$$

for some constant $\beta > 0$. Testing Eq. (A.53) with $\boldsymbol{v} \in \boldsymbol{H}_0^1(\Omega)$, we have

$$(\nabla p, \boldsymbol{v})_\Omega = (\boldsymbol{f}, \boldsymbol{v})_\Omega + (\mu \Delta \boldsymbol{u}, \boldsymbol{v})_\Omega.$$

Integrating by parts, dividing by $\|\boldsymbol{v}\|_{H^1(\Omega)}$ and taking the supremum:

$$\begin{aligned}\sup \frac{(p, \nabla \cdot \boldsymbol{v})}{\|\boldsymbol{v}\|_{H^1(\Omega)}} &= \sup \left\{ \frac{(\boldsymbol{f}, \boldsymbol{v})}{\|\boldsymbol{v}\|_{H^1(\Omega)}} - \frac{\mu(\nabla \boldsymbol{u}, \nabla \boldsymbol{v})}{\|\boldsymbol{v}\|_{H^1(\Omega)}} \right\} \\ &\leq \frac{\|\boldsymbol{f}\| \|\boldsymbol{v}\|_{L^2}}{\|\boldsymbol{v}\|_{H^1(\Omega)}} + \mu \|\nabla \boldsymbol{u}\| \leq \|\boldsymbol{f}\| + \mu \frac{C_P}{\mu} \|\boldsymbol{f}\| = (1 + C_P) \|\boldsymbol{f}\|.\end{aligned}$$

By the inf–sup condition, we then have $\|p\| \leq \frac{1+C_P}{\beta} \|\boldsymbol{f}\|$, bounding p, as required.

$\boldsymbol{f} = \boldsymbol{0}, g = 0, \boldsymbol{h} \neq \boldsymbol{0}$. In this case, we have

$$-\nabla \cdot \boldsymbol{\sigma} + \nabla p = \boldsymbol{0} \quad \text{in } \Omega, \tag{A.63}$$

$$\nabla \cdot \boldsymbol{u} = 0 \quad \text{in } \Omega, \tag{A.64}$$

$$\frac{1}{\mu}\boldsymbol{\sigma} - \nabla \boldsymbol{u} = \boldsymbol{h} \quad \text{in } \Omega, \tag{A.65}$$

$$\boldsymbol{u} = \boldsymbol{0} \quad \text{on } \partial\Omega. \tag{A.66}$$

Then, $\boldsymbol{\sigma} = \mu(\nabla \boldsymbol{u} + \boldsymbol{h})$, and we have:

$$-\nabla \cdot \boldsymbol{\sigma} + \nabla p = -\mu \Delta \boldsymbol{u} - \mu \nabla \cdot \boldsymbol{h} + \nabla p = \boldsymbol{0},$$

so that

$$-\mu \Delta \boldsymbol{u} + \nabla p = -\mu \nabla \cdot \boldsymbol{h}$$

in a distributional sense. Testing with $\boldsymbol{u}$, and integrating the left hand side by parts, again the pressure term vanishes because $\nabla \cdot \boldsymbol{u} = 0$, so that much as before, we obtain:

$$\begin{aligned}\mu(\nabla \boldsymbol{u}, \nabla \boldsymbol{u})_\Omega &= \mu(\nabla \cdot \boldsymbol{h}, \boldsymbol{u})_\Omega \\ &= -\mu(\boldsymbol{h}, \nabla \boldsymbol{u})_\Omega \leq \mu \|\boldsymbol{h}\|_{L^2(\Omega)} \|\nabla \boldsymbol{u}\|_{L^2(\Omega)}.\end{aligned}$$

So $\|\nabla \boldsymbol{u}\| \leq \|\boldsymbol{h}\|$, and the bounds $\|\boldsymbol{u}\| \leq C_P \|\boldsymbol{h}\|$ and $\|p\| \leq \frac{\mu}{\beta}(\|\nabla \boldsymbol{u}\| + \|\boldsymbol{h}\|) \leq \frac{2\mu}{\beta}\|\boldsymbol{h}\|$ can be established in a similar fashion as above.

$\boldsymbol{f} = \boldsymbol{0}, g \neq 0, \boldsymbol{h} = \boldsymbol{0}$. In this case, we have

$$-\nabla \cdot \boldsymbol{\sigma} + \nabla p = \boldsymbol{0} \quad \text{in } \Omega, \tag{A.67}$$

$$\nabla \cdot \boldsymbol{u} = g \quad \text{in } \Omega, \tag{A.68}$$

$$\frac{1}{\mu}\boldsymbol{\sigma} - \nabla \boldsymbol{u} = 0 \quad \text{in } \Omega, \tag{A.69}$$

$$\boldsymbol{u} = \boldsymbol{0} \quad \text{on } \partial\Omega. \tag{A.70}$$

We must also assume compatibility between g and the boundary condition on $\boldsymbol{u}$; that is, that g has zero average on Ω:

$$\int_\Omega g = \int_{\partial\Omega} \boldsymbol{u} \cdot \boldsymbol{n} = 0.$$

The inf–sup condition (A.62) is equivalent[23] to the existence, for every $g \in L^2(\Omega)$, of $\boldsymbol{u}_0 \in H_0^1$ such that

$$\nabla \cdot \boldsymbol{u}_0 = g \quad \text{and} \quad \|\boldsymbol{u}_0\| \leq C \|g\| .$$

Defining $\boldsymbol{w} \in H_0^1$ by $\boldsymbol{w} = \boldsymbol{u} - \boldsymbol{u}_0$, we substitute $\boldsymbol{u} = \boldsymbol{w} + \boldsymbol{u}_0$ into the system (A.67)–(A.70), obtaining

$$\begin{aligned}
&-\nabla \cdot \boldsymbol{\sigma} + \nabla p = \boldsymbol{0} \quad \text{in } \Omega, \\
&\nabla \cdot \boldsymbol{w} = \nabla \cdot (\boldsymbol{u} - \boldsymbol{u}_0) = 0 \quad \text{in } \Omega, \\
&\frac{1}{\mu}\boldsymbol{\sigma} - \nabla \boldsymbol{w} = \nabla \boldsymbol{u}_0 \quad \text{in } \Omega, \\
&\boldsymbol{w} = \boldsymbol{0} \quad \text{on } \partial\Omega .
\end{aligned}$$

Thus we have reduced the $g \neq 0$ case to the $\boldsymbol{h} \neq 0$ case. This completes the proof.

References

[1] L. Demkowicz, J. Gopalakrishnan, A class of discontinuous Petrov–Galerkin methods, part I: the transport equation, Comput. Methods Appl. Mech. Engrg. 199 (2010) 1558–1572. See also ICES Report 2009–12.
[2] L. Demkowicz, J. Gopalakrishnan, A class of discontinuous Petrov–Galerkin methods, part II: optimal test functions, Numer. Methods Partial Differential Equations 27 (1) (2011) 70–105, in print.
[3] C.L. Bottasso, S. Micheletti, R. Sacco, The discontinuous Petrov–Galerkin method for elliptic problems, Comput. Methods Appl. Mech. Engrg. 191 (2002) 3391–3409.
[4] C.L. Bottasso, S. Micheletti, R. Sacco, A multiscale formulation of the discontinuous Petrov–Galerkin method for advective–diffusive problems, Comput. Methods Appl. Mech. Engrg. 194 (2005) 2819–2838.
[5] J. Zitelli, I. Muga, L. Demkowicz, J. Gopalakrishnan, D. Pardo, V. Calo, A class of discontinuous Petrov–Galerkin methods, part IV: wave propagation problems, J. Comput. Phys. 230 (2011) 2406–2432.
[6] J. Bramwell, L. Demkowicz, W. Qiu, Solution of dual-mixed elasticity equations using Arnold–Falk–Winther element and discontinuous Petrov–Galerkin method, a comparison, (2010-23), 2010.
[7] A.H. Niemi, J.A. Bramwell, L.F. Demkowicz, Discontinuous Petrov–Galerkin method with optimal test functions for thin-body problems in solid mechanics, Comput. Methods Appl. Mech. Eng. 200 (9–12) (2011) 1291–1300.
[8] N.V. Roberts, D. Ridzal, P.N. Bochev, L. Demkowicz, K.J. Peterson, Ch.M. Siefert, Application of a discontinuous Petrov–Galerkin method to the Stokes equations, in: CSRI Summer Proceedings 2010, 2010.
[9] L. Demkowicz, J. Gopalakrishnan, Analysis of the DPG method for the Poisson problem, SIAM J. Numer. Anal. 49 (5) (2011) 1788–1809.
[10] L. Demkowicz, N. Heuer, Robust DPG Method for Convection-Dominated Diffusion Problems, Technical Report 33, ICES, 2011.
[11] Tan Bui-Thanh, Leszek Demkowicz, Omar Ghattas, A unified discontinuous Petrov–Galerkin method and its analysis for Friedrichs' systems, SIAM J. Numer. Anal. (2011) submitted for publication. Also ICES Report ICES-11-34, November 2011.
[12] J. Chan, L. Demkowicz, R. Moser, N. Roberts, A Class of Discontinuous Petrov–Galerkin Methods, Part V: Solution of 1D Burgers and Navier–Stokes Equations, No. 25, ICES, 2010.
[13] Jay Gopalakrishnan, Weifeng Qiu, An Analysis of the Practical DPG Method, Technical Report, 2011, arXiv:1107.4293.
[14] W. Dahmen, Ch. Huang, Ch. Schwab, G. Welper, Adaptive Petrov Galerkin methods for first order transport equations, SIAM J. Numer. Anal. 50 (5) (2012) 2420–2445. See also Institut fuer Geometrie und Praktische Mathematik, Technical Report 2011/321.
[15] D. Moro, N.C. Nguyen, J. Peraire, A hybridized discontinuous Petrov–Galerkin scheme for scalar conservation laws, Internat. J. Numer. Methods Engrg. 91 (9) (2012) 950–970.
[16] Nathan V. Roberts, Denis Ridzal, Pavel B. Bochev, Leszek D. Demkowicz, A Toolbox for a Class of Discontinuous Petrov–Galerkin Methods Using Trilinos, Technical Report SAND2011-6678, Sandia National Laboratories, 2011.
[17] D. Boffi, F. Brezzi, M. Fortin, Finite elements for the Stokes problem, in: Lecture Notes in Mathematics, vol. 1939, Springer, 2008, pp. 45–100.
[18] F. Brezzi, On the existence, uniqueness, and approximation of saddle point problems arising from Lagrangian multipliers, RAIRO Modél. Math. Anal. Numér. 2 (1974) 129–151.
[19] O.A. Ladyzhenskaya, The Mathematical Theory of Viscous Incompressible Flows, Gordon and Breach, London, 1969.
[20] P. Castillo, B. Cockburn, I. Perugia, D. Schötzau, An a priori error analysis of the local discontinuous Galerkin method for elliptic problems, SIAM J. Numer. Anal. 38 (2000) 1676–1706.
[21] B. Cockburn, G. Kanschat, D. Schotzau, Ch. Schwab, Local discontinuous Galerkin methods for the Stokes system, SIAM J. Numer. Anal. 40 (2003) 319–343.
[22] J. Bramwell, L. Demkowicz, J. Gopalakrishnan, W. Qiu, A locking-free *hp* DPG method for linear elasticity with symmetric stresses, Numer. Math. 122 (4) (2012) 671–707.
[23] L. Demkowicz, J. Gopalakrishnan, I. Muga, J. Zitelli, Wavenumber explicit analysis for a DPG method for the multidimensional Helmholtz equation, Comput. Methods Appl. Mech. Engrg. 213–216 (2012) 126–138.
[24] T. Bui-Thanh, L. Demkowicz, O. Ghattas, A Unified Discontinuous Petrov–Galerkin Method and its Analysis for Friedrichs' Systems, No. 34, ICES, 2011.
[25] W. McLean, Strongly Elliptic Systems and Boundary Integral Equations, Cambridge University Press, 2000.
[26] R.E. Showalter, Hilbert Space Methods for Partial Differential Equations, Pitman Publishing Limited, London, 1977.
[27] J.T. Oden, L.F. Demkowicz, Applied Functional Analysis for Science and Engineering, second ed., Chapman & Hall/CRC Press, Boca Raton, 2010.
[28] L. Demkowicz, Computing with *hp* Finite Elements, I. One- and Two-Dimensional Elliptic and Maxwell Problems, Chapman & Hall/CRC Press, Taylor and Francis, 2006.
[29] Kurt O. Friedrichs, Symmetric positive linear differential equations, Comm. Pure Appl. Math. XI (1958) 333–418.
[30] Alexandre Ern, Jean-Luc Guermond, Gilbert Caplain, An intrinsic criterion for the bijectivity of Hilbert operators related to Friedrichs' systems, Comm. Partial Differential Equations 32 (2) (2007) 317–341.
[31] Kôsaku Yosida, Functional Analysis, Springer, 1980.
[32] Leszek F. Demkowicz, Babuška <=> Brezzi ?? Technical Report 06-08, ICES, 2006.
[33] Pavel Bochev, R.B. Lehoucq, On the finite element solution of the pure Neumann problem, SIAM Rev. 47 (1) (2005) 55–66.

[23] Again, see Section 2.2 of [37].

[34] Michael A. Heroux, Roscoe A. Bartlett, Vicki E. Howle, Robert J. Hoekstra, Jonathan J. Hu, Tamara G. Kolda, Richard B. Lehoucq, Kevin R. Long, Roger P. Pawlowski, Eric T. Phipps, Andrew G. Salinger, Heidi K. Thornquist, Ray S. Tuminaro, James M. Willenbring, Alan Williams, Kendall S. Stanley, An overview of the Trilinos project, ACM Trans. Math. Software 31 (3) (2005) 397–423.
[35] Bernardo Cockburn, Guido Kanschat, Dominik Schötzau, Christoph Schwab, Local discontinuous Galerkin methods for the Stokes system, SIAM J. Numer. Anal. 40 (1) (2003) 319–343.
[36] H.K. Moffatt, Viscous and resistive eddies near a sharp corner, J. Fluid Mech. 18 (1) (1964) 1–18.
[37] Martin Costabel, Monique Dauge, On the inequalities of Babuška-Aziz, Friedrichs and Horgan-Payne, http://arxiv.org/abs/1303.6141.